U.S. Department of Transportation

Federal Railroad Administration

Field Demonstration of Geocell Track Substructure Support System Under High-Speed Passenger Railroad Operations

Office of Research,
Development
and Technology
Washington, DC 20590

REPORT DOCUMENTATION PAGE

Form Approved
OMB No. 0704-0188

1. AGENCY USE ONLY (Leave blank)	2. REPORT DATE July 2018	3. REPORT TYPE AND DATES COVERED Technical Report, 2012–2017

4. TITLE AND SUBTITLE Field Demonstration of Geocell Track Substructure Support System Under High-Speed Passenger Railroad Operations	5. FUNDING NUMBERS DTFR53-15-C-00019
6. AUTHOR(S) Joseph Palese PE, MCE[1], Christopher M. Hartsbough[1], Dr. Allan M Zarembski PE, FASME, Hon Mbr[2], Dr. Hoe I. Ling[3]	

7. PERFORMING ORGANIZATION NAME(S) AND ADDRESS(ES) Harsco Rail[1] 2401 Edmund Rd West Columbia, SC 29170-1931 University of Delaware[2] Office of Sponsored Programs 210 Hullihen Hall Newark, DE 19716 Columbia University[3] 500 W 120th St New York, NY 10027	8. PERFORMING ORGANIZATION REPORT NUMBER

9. SPONSORING/MONITORING AGENCY NAME(S) AND ADDRESS(ES) U.S. Department of Transportation Federal Railroad Administration Office of Railroad Policy and Development Office of Research, Development and Technology Washington, DC 20590	10. SPONSORING/MONITORING AGENCY REPORT NUMBER DOT/FRA/ORD-18/27

11. SUPPLEMENTARY NOTES
COR: Hugh Thompson

12a. DISTRIBUTION/AVAILABILITY STATEMENT This document is available to the public through the FRA Web site at http://www.fra.dot.gov.	12b. DISTRIBUTION CODE

13. ABSTRACT (Maximum 200 words)

Regions of track, which experience high rates of track geometry degradation, tend to require frequent maintenance interventions that are typically surfacing or tamping. Harsco Rail and the University of Delaware conducted a survey regarding this costly process that involved both machine time and track time to complete. A region of track on Amtrak's Northeast Corridor (NEC) (Oakington Road, Havre de Grace, MD—Milepost 63.7) was selected to have a geocell-based subgrade stabilizing material installed as part of a subgrade renewal project. This report describes the renewal of the track region as well as the experimental setup, data, and results used to quantify the effectiveness of the geocell material and maintenance activity.

14. SUBJECT TERMS Track geometry, high-speed track, track quality index, TQI, ballast, sub-ballast, subgrade, Surfacing Cycle, geocell, Neoweb™, Amtrak, Northeast Corridor, NEC	15. NUMBER OF PAGES 79
	16. PRICE CODE

17. SECURITY CLASSIFICATION OF REPORT Unclassified	18. SECURITY CLASSIFICATION OF THIS PAGE Unclassified	19. SECURITY CLASSIFICATION OF ABSTRACT Unclassified	20. LIMITATION OF ABSTRACT

NSN 7540-01-280-5500

Standard Form 298 (Rev. 2-89)
Prescribed by
ANSI Std. 239-18
298-102

METRIC/ENGLISH CONVERSION FACTORS

ENGLISH TO METRIC

METRIC TO ENGLISH

LENGTH (APPROXIMATE)

1 inch (in)	=	2.5 centimeters (cm)
1 foot (ft)	=	30 centimeters (cm)
1 yard (yd)	=	0.9 meter (m)
1 mile (mi)	=	1.6 kilometers (km)

LENGTH (APPROXIMATE)

1 millimeter (mm)	=	0.04 inch (in)
1 centimeter (cm)	=	0.4 inch (in)
1 meter (m)	=	3.3 feet (ft)
1 meter (m)	=	1.1 yards (yd)
1 kilometer (km)	=	0.6 mile (mi)

AREA (APPROXIMATE)

1 square inch (sq in, in^2)	=	6.5 square centimeters (cm^2)
1 square foot (sq ft, ft^2)	=	0.09 square meter (m^2)
1 square yard (sq yd, yd^2)	=	0.8 square meter (m^2)
1 square mile (sq mi, mi^2)	=	2.6 square kilometers (km^2)
1 acre = 0.4 hectare (he)	=	4,000 square meters (m^2)

AREA (APPROXIMATE)

1 square centimeter (cm^2)	=	0.16 square inch (sq in, in^2)
1 square meter (m^2)	=	1.2 square yards (sq yd, yd^2)
1 square kilometer (km^2)	=	0.4 square mile (sq mi, mi^2)
10,000 square meters (m^2)	=	1 hectare (ha) = 2.5 acres

MASS - WEIGHT (APPROXIMATE)

1 ounce (oz)	=	28 grams (gm)
1 pound (lb)	=	0.45 kilogram (kg)
1 short ton = 2,000 pounds (lb)	=	0.9 tonne (t)

MASS - WEIGHT (APPROXIMATE)

1 gram (gm)	=	0.036 ounce (oz)
1 kilogram (kg)	=	2.2 pounds (lb)
1 tonne (t)	=	1,000 kilograms (kg)
	=	1.1 short tons

VOLUME (APPROXIMATE)

1 teaspoon (tsp)	=	5 milliliters (ml)
1 tablespoon (tbsp)	=	15 milliliters (ml)
1 fluid ounce (fl oz)	=	30 milliliters (ml)
1 cup (c)	=	0.24 liter (l)
1 pint (pt)	=	0.47 liter (l)
1 quart (qt)	=	0.96 liter (l)
1 gallon (gal)	=	3.8 liters (l)
1 cubic foot (cu ft, ft^3)	=	0.03 cubic meter (m^3)
1 cubic yard (cu yd, yd^3)	=	0.76 cubic meter (m^3)

VOLUME (APPROXIMATE)

1 milliliter (ml)	=	0.03 fluid ounce (fl oz)
1 liter (l)	=	2.1 pints (pt)
1 liter (l)	=	1.06 quarts (qt)
1 liter (l)	=	0.26 gallon (gal)
1 cubic meter (m^3)	=	36 cubic feet (cu ft, ft^3)
1 cubic meter (m^3)	=	1.3 cubic yards (cu yd, yd^3)

TEMPERATURE (EXACT)

$[(x-32)(5/9)]$ °F $=$ y °C

TEMPERATURE (EXACT)

$[(9/5)\, y + 32]$ °C $=$ x °F

QUICK INCH - CENTIMETER LENGTH CONVERSION
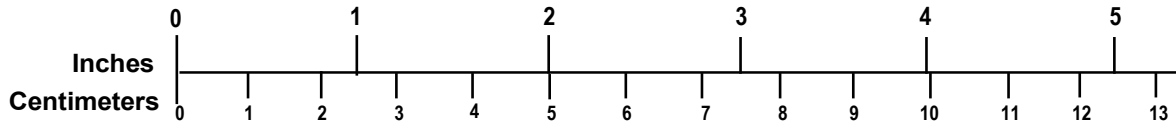
QUICK FAHRENHEIT - CELSIUS TEMPERATURE CONVERSION
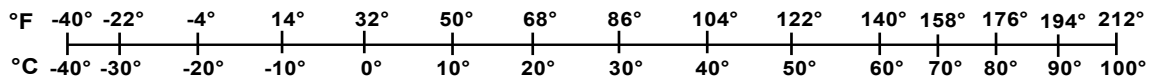
For more exact and or other conversion factors, see NIST Miscellaneous Publication 286, Units of Weights and Measures. Price $2.50 SD Catalog No. C13 10286   **Updated 6/17/98**

ii

Acknowledgements

The authors would like to acknowledge the following individuals for their contributions and support to this project:

Contents

Illustrations

Tables

Executive Summary

From 2012 through 2017, the Federal Railroad Administration provided funding to Harsco Rail and the University of Delaware to conduct a study on a region of Amtrak's Northeast Corridor where regions of track that experience high rates of track geometry degradation tend to require frequent maintenance interventions, typically surfacing or tamping where this can be a costly process. In the case of high-speed track where track geometry tolerances are very strict, frequent maintenance cycles can become quite burdensome.

This region of track (Oakington Road, Havre de Grace, MD—Milepost [MP] 63.7) was selected to have a geocell-based subgrade stabilizing material installed as part of a subgrade renewal project. The expectations of this material were to decrease the degradation of track geometry as well as decrease ballast/subgrade interface pressure and increase surfacing cycle. A testing plan was developed to monitor and evaluate the geocell material to determine if it is a valid means of controlling track geometry degradation and if it is cost effective for the results achieved. To do this, pressure transducers were installed below the left and right rails at the ballast/sub-ballast interface both inside and outside of regions of track where the geocell was installed. Pressure reading was monitored at predefined intervals over a 7-month period after completion of track maintenance. In addition to pressure data, monthly track geometry data was also supplied by Amtrak and analyzed to look at changes in the rate of track geometry degradation association with the installation of the geocell material.

Analysis of the pressure and track geometry data showed that the geocell material was very effective in minimizing and controlling track geometry degradation. After installation, interface pressure in the geocell region of track was roughly half of the measurements made outside of the geocell zone. With respect to track geometry degradation, analysis of the track condition, as defined by the track quality index (TQI), showed that the geocell region had a measurably reduced rate of degradation.. This, in turn, translates into a corresponding extension of maintenance (surfacing) cycles.

Thus, by utilizing a geocell-based subgrade stabilizing material on a location of high-speed track showing significant historic geometry degradation, it was shown that an increase in surfacing cycle by a factor of 6.7 can be realized. A cost benefit analysis was done to determine the return on investment (ROI) of installing the geocell material. For the current location, an ROI of nearly 113 percent was realized by installing the geocell material. This report describes the renewal of the track region as well as the experimental setup, data, and results used to quantify the effectiveness of the geocell material and maintenance activity.

1. Introduction

Harsco Rail and the University of Delaware conducted a survey sponsored by the Federal Railroad Administration (FRA) to investigate ballast fouling and associated degradation of track geometry, as indicated by the track quality index (TQI) in Figure 1, that this is a serious problem for railway systems in general and high-speed passenger rail systems. This is the case for Amtrak's Northeast Corridor (NEC) where a historical problem area existed near Oakington Road, Havre de Grace, MD, in the vicinity of Milepost (MP) 63.7 between Philadelphia, PA, and Washington, DC. The original problem seems to have developed after the undercutting of the middle track, Track 3, was performed in the 1990s as part of a double stack clearance project. This undercutting appeared to have impinged upon an underlying clay layer beneath the track with the result that fouling and drainage problems developed in the area of Oakington Road, MP 63.7. Over time the ballast became fouled with clay, and after rain, would become muddy, as illustrated in Figure 2 and Figure 3.
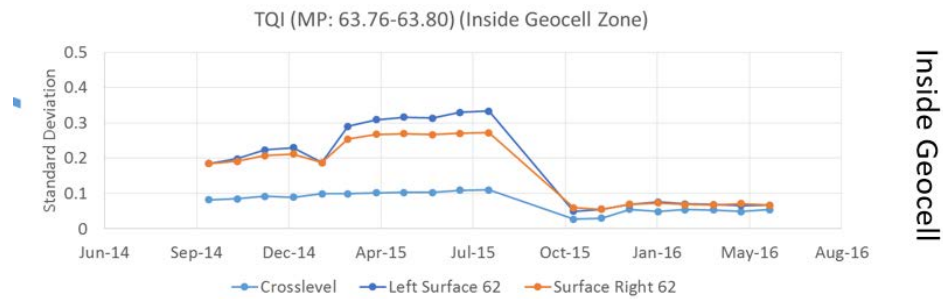
Figure 1: Track Geometry Degradation Rate Before and After Geocell Installation
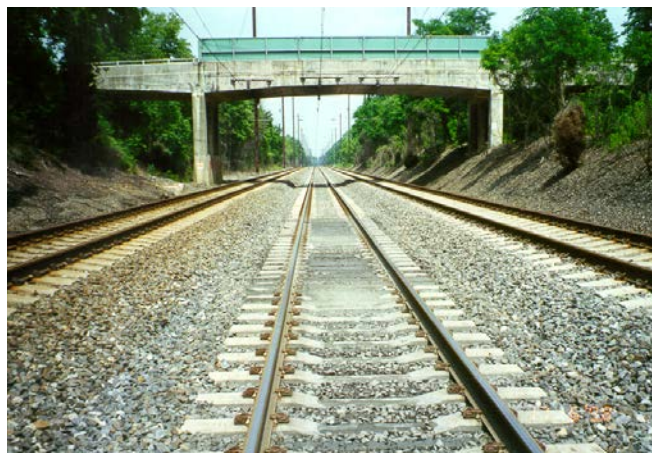
Figure 2: Fouling and Mud Spots at Oakington Road; 1998

Figure 3: Fouling and Mud Spots at Oakington Road; 2010

In addition, the clay has been migrating to the adjacent high-speed tracks with the result that frequent surfacing has been required on these key high-speed tracks.

1.1   Background

Maintaining track geometry is a key element in the maintenance of railroad track structure, particularly for high-speed passenger operations. In locations with poor subgrade (parent soil) and/or poor ballast conditions, track geometry degrades rapidly resulting in the need for frequent expensive maintenance, such as surfacing and other ballast maintenance activities. Track geometry maintenance, to include surfacing, ballast cleaning, and related maintenance activities, represents one of the three major maintenance cost areas for the track structure. In the case of high-speed rail, it is often the largest single maintenance cost area, since the geometry requirements for high-speed rail are extremely tight, with little tolerance for degradation. This in turn, results in the need for frequent surfacing to maintain these tight geometry standards. In the location of poor track substructure, due to either weak or water susceptible soils or fouled ballast, the rate of surface degradation is increased with the need for frequent surface maintenance resulted in high costs and the loss of track time for train operations due to the maintenance activities.

The new generation of geotechnical materials based on three-dimensional cellular confinement system technology (geocells) provides reinforcement to the substructure and serves as a structural support element at the ballast/subgrade interface in railroad track. The use of this geocell materials, placed under the ballast layer, usually at the ballast/subgrade interface area has been shown to decrease the rate of track surface geometry degradation (both surface and cross-level) under a range of traffic loadings. The availability of a proven effective way to reduce the rate of degradation, particularly in these high degradation rate locations, will be of great value and could be adopted both in the construction of new lines and in the maintenance of existing lines.

The use of geotechnical (geosynthetic) materials to provide reinforcement of soil materials under highways and related systems is a mature technology. The application of these materials to railways with their high stress levels and service requirements is relatively new and untried.

Earlier geosynthetic materials such as geotextiles did not live up to their initial expectations and did not provide the improvements originally envisioned.

Geocells were first developed in the late 1970's as a three-dimensional cellular structure designed to confine soils (Alford S. J., and Webster, S. L., 1977). Geocells were typically made of high density polyethylene (HDPE) materials. They can be collapsed and transported easily to the construction sites. Installations are rapid and only light equipment is needed. There are many successful cases of application of geocells in unpaved roadways that reduced surface rutting (Han et al., 2008). Additionally, geocells have also been found to give excellent performance as retaining walls.

Application of geocells in railway track, particularly in the ballast/subgrade layer is relatively recent and has been limited to date. Early testing at Transportation Technology Center, Inc. (TTCI) in Pueblo, CO, showed promise in soft subgrade conditions together with limited testing and applications in South Africa, Japan, Russia, United Kingdom, and Israel (Chrismer, S., 1999). In order to investigate the effectiveness of the stiffer and less temperature sensitive Novel Polymeric Alloy (NPA) geocells in reinforcing the ballast,[1] a series of monotonic and cyclic loading tests were conducted on a sandstone ballast embankment at Columbia University in the period of 2009–2012 (Leshchinsky et al., 2010, 2013). The significant improved performance compared to unreinforced embankments, such as reduction in vertical settlement and lateral spreading, was confirmed. Application of the geocells in the ballast/subgrade interface, results in the geocells generating a basic confinement of the subgrade material, which testing shows will result in an improvement in the mechanical behavior of any soil composition.

In the Columbia University testing of a geocell layer in the ballast, the geocells confine the ballast particles. When subjected to repeated vertical stress due to train loading, this confinement constrains movement of the individual ballast particles thus exhibiting stiffer reaction (i.e., less elastic settlement under given load). Moreover, because the particles are restrained, there is less abrasion and/or plastic deformation of the ballast. Confinement also increases the apparent strength of the composite ballast-geocells. All these factors appear to reduce the rate of ballast degradation as well as track geometry loss.

The materials used in manufacturing geocells can be very important because longer lived materials with minimum creep preserve the cells' geometry and enhance (and maintain) the confinement effects. This is of particular importance in the railroad environment, especially within the ballast, which is a harsh environment for any geosynthetic material. Better confinement means very little movement of ballast particles confined within the three-dimensional cells when subjected to repeated train loading, thus insuring less abrasion of ballast as well as to the walls of the geocell material. Creep resistant geocell materials also provide for longer term performance.

The latest generation of geotechnical materials based on three-dimensional cellular confinement system technology (geocells) shows significant promise in being able to provide reinforcement to the substructure and serve as a structural support element at the ballast/subgrade interface in railroad track. Laboratory testing such as the recent test program at Columbia University and preliminary field testing such as at TTCI in Pueblo and in some overseas test locations (e.g.,

---

[1] The use of the old generation HDPE geocells for reinforcement of the ballast is questionable because of the relatively high polymeric creep of the HDPE.

South Africa) have shown reductions in rate of degradation (corresponding to extension in surfacing intervention cycles) ranging from factors of 1.7 to 5+ under very controlled conditions (Chrismer, S., 1997) (Kae, J. K., 2007) (Leshinsky, B. et al., 2010, 2013).

1.2   Objectives

This report presents the results of a research study looking at the application of a new generation of three-dimensional cellular confinement systems (geocells)[2] in reducing the rate of track geometry degradation, particularly in poor subgrade and ballast locations which require frequent and expensive track surface maintenance.

1.3   Overall Approach

The research activities included load cell monitoring and track geometry degradation trending on Amtrak's NEC Main Line. The project specifically focused on resolving subgrade instability beneath tracks two and three in the area of the Oakington Road bridge, located in Havre de Grace, MD, through the use of geocell material reinforced with granular stone material. Monitoring and subsequent trending analysis was conducted over a 5-year span.

1.3.1   Oakington Road Site

The test site for this activity was on Amtrak's NEC Main Line—Mid-Atlantic Division, NEC AP-Line, MP 63.7, at Oakington Road, Havre de Grace, MD, as shown in Figure 4. As shown previously in Figure 2 and Figure 3, this site has ballast fouling and develops significant mud-spots, particularly after rain. The original problem seems to have developed after undercutting of the middle track, Track 3, was performed in the 1990s as part of a double stack clearance project. This undercutting appeared to have impinged upon an underlying clay layer beneath the track with the result that fouling and drainage problems developed in the area of Oakington Road, MP 63.7.

---

[2] The specific geocell material used in this research project was Neoweb™, a product of PRS Mediterranean Ltd. of Tel Aviv, Israel.
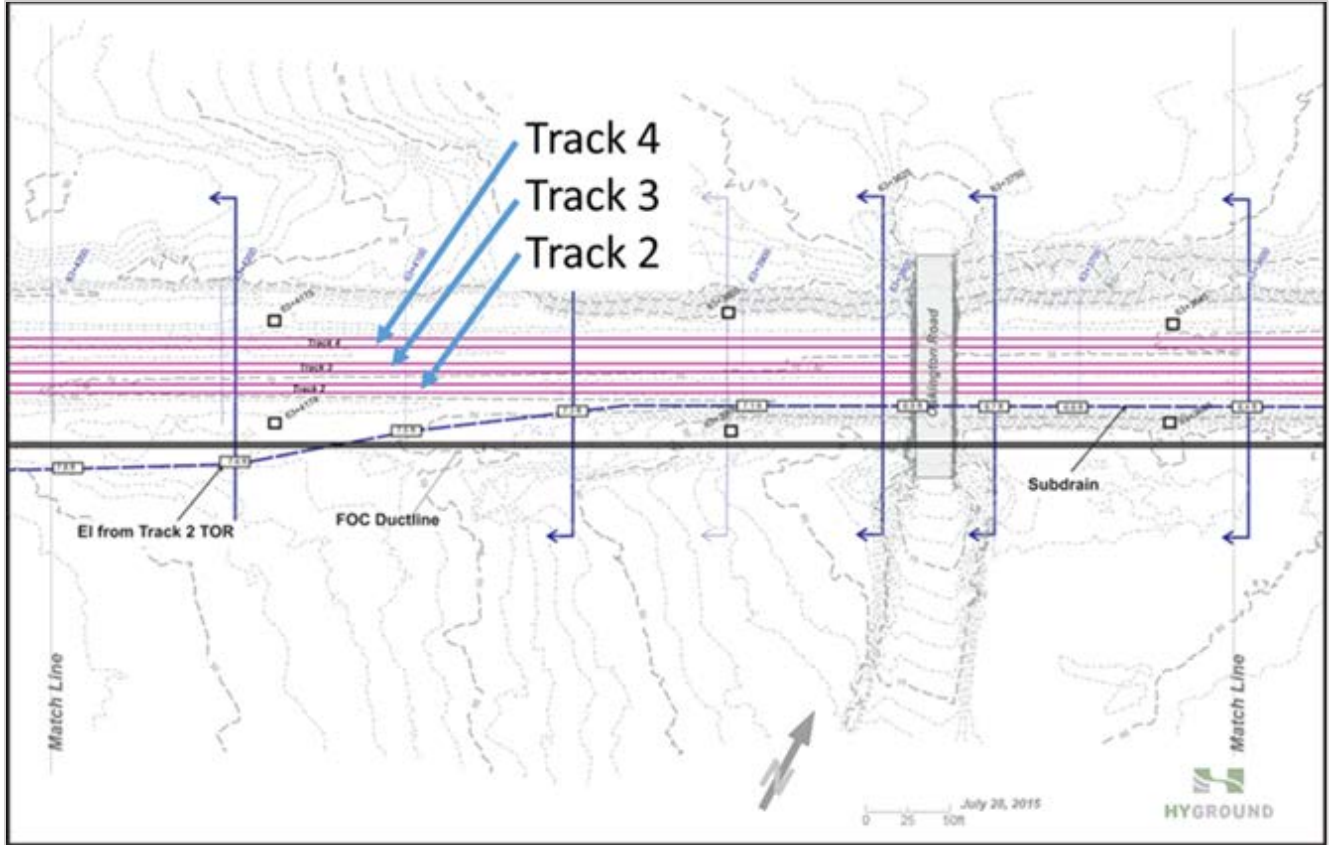
Figure 4: Track Chart: Oakington Road

Traffic includes high-speed Acela service, conventional and regional rail service, and occasional freight traffic (see Figure 5). Because the traffic includes high-speed passenger operations, the track is FRA Class 7 with a maximum authorized speed of 125 mph. This requires frequent track maintenance because of the very tight track geometry limits for this class of track. The presence of the clay in the ballast and the development of mud spots result in more rapid degradation of the track geometry and the need for more frequent surfacing, an expensive activity.

Figure 5: Mix of High-Speed and Conventional Passenger Train Operations

Testing at this site has shown that this is a location with known soil problems including highly plastic clay, which has been shown to be a particularly weak subgrade. Significant information is available about this sites soil condition and history of track geometry degradation to include extensive track geometry history data.

Figure 6 shows a typical cross section of the three tracks in this area. Figure 7 shows a cross-trench used to investigate the soil condition. Note the poor condition of the clay subgrade.

Typical Cross-section
MP63 + 3900'

2 U/C passes to lower
Track 2

Most unstable subgrade
Track 3

Track 4

Section MP63 + 3900'
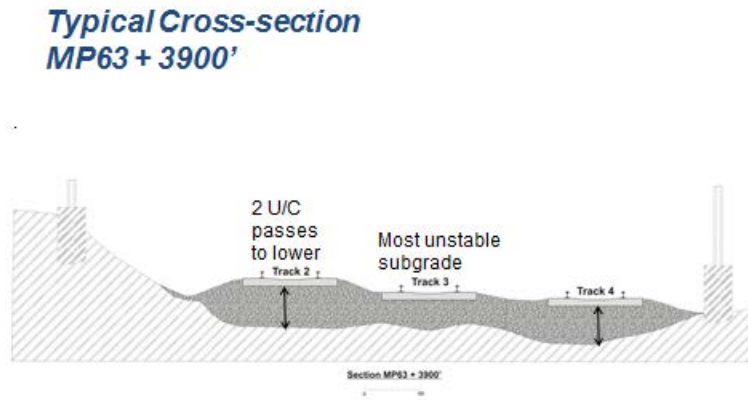
Updated 8/13/11

Figure 6: Typical Cross-Section

11 12 '96

Figure 7: Cross-Trench for Soil Investigation

Cone penetrometer testing was used to measure soil strength in this area in the mid-1990s. Cone penetrometer tests use the tip resistance, i.e., the resistance at the tip of the cone, to determine soil condition. Figure 8 shows the results of the cone penetrometer test under Track 3 at Oakington Road. The resistance of the ballast, and in particular the top 2 feet of the ballast had lower than expected resistance, with a maximum of ~2,000 psi as opposed to the expected resistance of between 5,000 to 6,000 psi which is typical for good clean ballast. The next 10 feet of clay had very low resistance, with a very low measured tip resistance of ~175 psi. This poor subgrade condition was subsequently confirmed by subsequent ground penetrating radar (GPR) measurements of the site.

Figure 9 shows an overlay of the cone penetrometer measurements on the track profile to show the areas of weak performing ballast and subgrade.

AMTRAK Site 27 Track 3
(MP 63.7) A27C3

Tip Resistance (psi)

Weaker Subgrade Portion
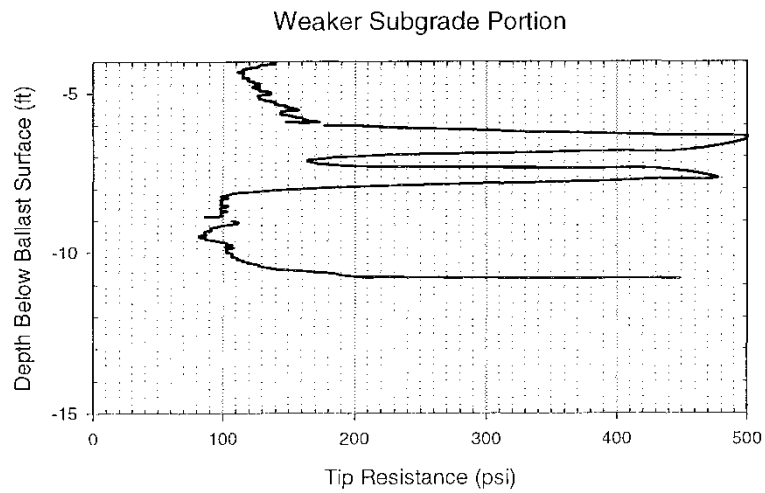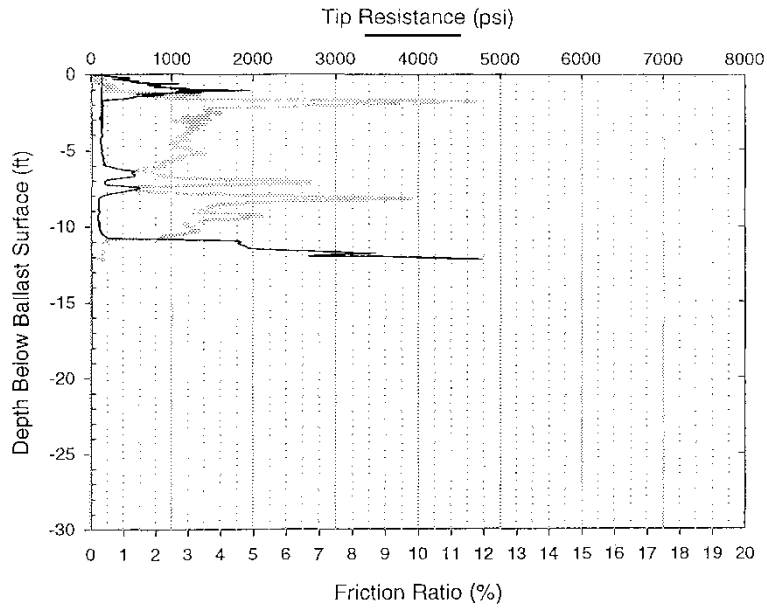
Figure 8: Cone Penetrometer Tests at Oakington Road

9

Cone penetrometer results from 1996

Figure 9: Overlay of Cone Penetrometer Measurements on Track Profile

GPR measurements support and expand on the cone penetrometer test results as shown in Figure 10. This includes the definition of the top of subgrade shown in Figure 11.
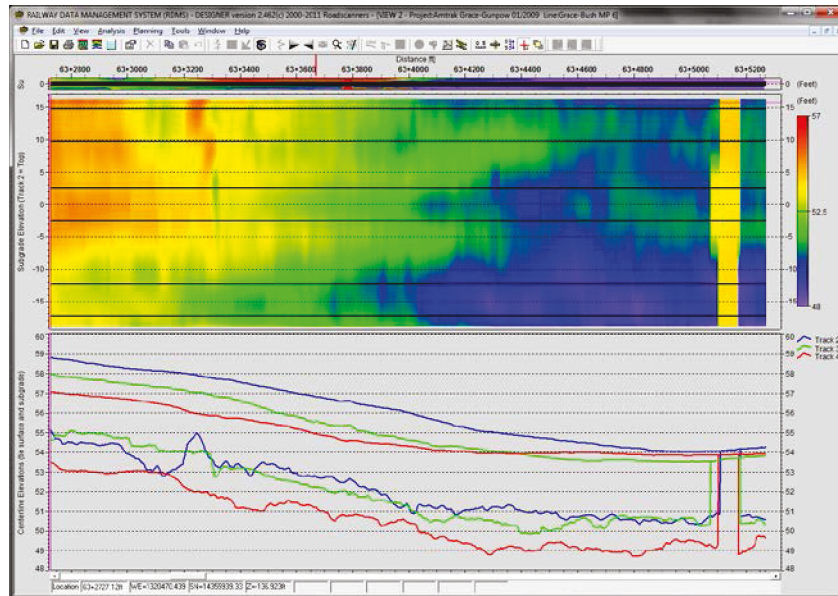
Figure 10: GPR Measurements and Track Surface Measurements (Track 2)

GPR provides subgrade elevation along track
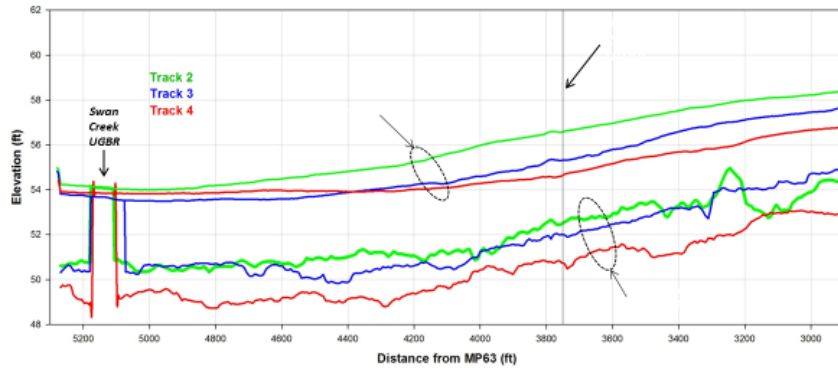
Figure 11: Subgrade Elevations for all Three Tracks from GPR Measurements

Likewise track geometry measurements show this zone in the vicinity of Oakington Road has a rapid rate of track geometry degradation. This is clearly illustrated in the overlay of three different geometry runs in Figure 12, Figure 13, and Figure 14 for Right Profile, Left Profile, and cross-level measurements, respectively. As can be seen, the center zone in the vicinity of Oakington Road experienced very rapid geometry degradation over a period of 8 months.
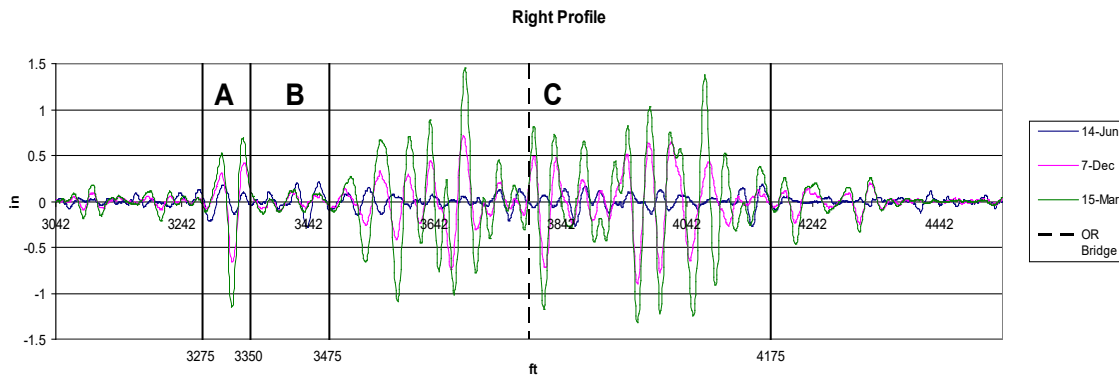
Figure 12: Right Profile Measurements (Three Runs Overlaid)

11
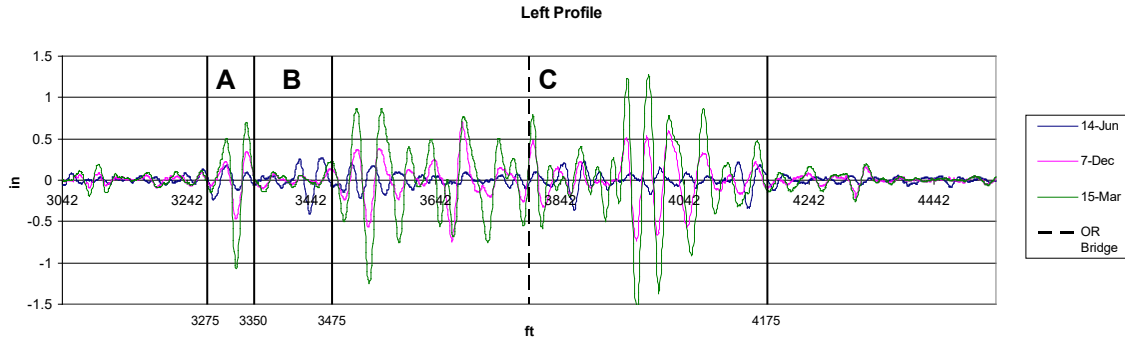
Figure 13: Left Profile Measurements (Three Runs Overlaid)
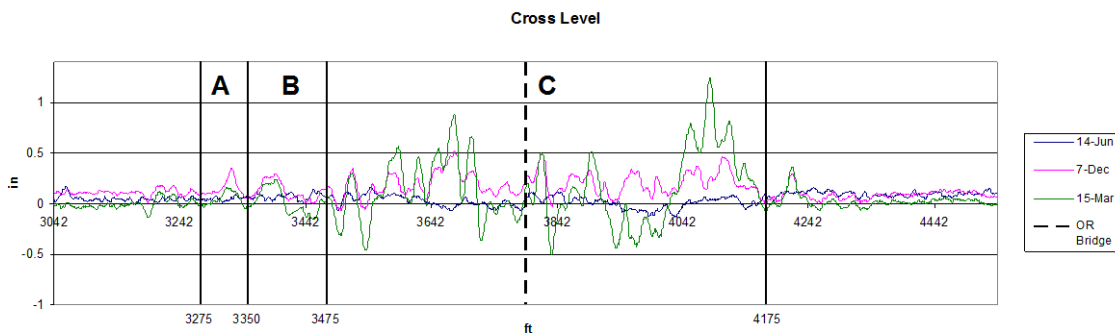
Figure 14: Cross-Level Measurements (Three Runs Overlaid)

Analysis of these geometry degradation zones led to three possible test options:

- Option 1) Install the geocell in section C only

- Option 2) Install the geocell in sections A and C

- Option 3) Install the geocell in all three sections (A, B, C)

Option 1 was determined to be the most cost effective and time efficient option, with a minimum track outage to disrupt traffic on the NEC. It also allowed for a portion of the track that experiences significant geometry degradation to be left as a "control" zone (Zone A) to compare performance with the zone in which the geocell is installed (Zone C). Note, it all leaves the ability to install additional geocell at a later time

1.4 Scope

As noted previously, the purpose of this test was to perform a full scale in-track field evaluation of geocell materials under actual main line track conditions on Amtrak track on the NEC. Specifically, track with a high rate of track geometry degradation and corresponding high level of track geometry maintenance was selected by Amtrak for testing. The selected location on MP 63.7 near Havre de Grace is an existing three track location with significant mud pumping and track geometry degradation, particularly in the center track (Track 3).

12

A geocell material, Neoweb™, was installed in the ballast/subgrade interface area to improve the strength of the poor performing soil. [3] This is accomplished by the geocell's working mechanism which confines the ballast particles within the cells of the Neoweb™ material. When subjected to repeated vertical stress due to train loading, this confinement constrains movement of the individual ballast particles thus exhibiting stiffer reaction (i.e., less elastic settlement under given load). Moreover, because the particles are restrained, there is less abrasion and/or plastic deformation of the ballast. Confinement also increases the apparent strength of the composite ballast-geocells. That is, due to increased confinement, the ballast bed exhibits higher strength. All these factors were expected to reduce the rate of ballast degradation as well as track geometry loss.

Thus, the purpose of this test is to examine and demonstrate the effectiveness of the geocells technology in reducing the rate of track geometry degradation, with the expectation that there will be an increase in surfacing cycle (reduction in rate of geometry degradation to failure) of the order of a factor of double or even more.

The original test plan was to install of the geocell material on the center track: Track 3. However, Amtrak was most concerned about the two high-speed tracks, Tracks 2 and 4 and subsequently shifted the focus of the test to Track 2 because of concern that the same type of ballast fouling/subgrade failure problems will occur on Track 2.

In addition to the installation of the geocell material in the test zone, undercutting of Track 2 occurred in spring 2015, with the goal of increasing clearances, since Track 2 has the highest elevation of all three tracks (see Figure 6 and Figure 11). In addition, drainage was improved in the test zone and in the adjacent tracks that were part of the upgrade and rehabilitation activity.

As a result, rehabilitation of approximately 2,400 feet of Track 2 was performed in September 2015. Approximately 800 feet of geocell material was installed in the center of the zone, around Oakington Road. In addition, Track 2 was shifted down approximately 18 inches (undercutting), and was shifted away from Track 3 approximately 18 inches. Also, as noted previously, additional drainage in the entire zone.

The installation was performed by Amtrak, with support by PRS Mediterranean Ltd. the supplier of the geocell material. Instrumentation was installed by a team consisting of Harsco Rail, Columbia University, and University of Delaware personnel.

1.5   Organization of the Report

This report is organized into the following 10 sections:

Section 1 is the introduction.

Section 2 provides the design of the test site that holds geocell material and the instrumentation of the test zones.

Section 3 describes the installation of geocell materials and load cells.

---

[3] The Neoloy® Neoweb™ Cellular Confinement System and its use are protected by US and other international patents. PRS Mediterranean Ltd. owns the rights to the Neoloy® and Neoweb™ patents. Neoweb™ and Neoloy® are registered trademarks of PRS Mediterranean Ltd.

Section 4 provides monitoring of the key track geometry parameters.

Section 5 presents the measurements and results of testing that was monitored over a 10-month time period.

Section 6 describes an economic life cycle benefit analysis.

Section 7 details a post-mortem of the test site containing the geocell material that was performed.

Section 8 provides a conclusion of the comparison of two distinct sets of track conditions that includes zones with and without a layer of Neocell™ geocell material.

2. Design of Test Site with Geocell Material

As noted above, the test site is Track 2 at MP 63.7 near Oakington Road, Havre de Grace, as shown in Figure 15 below. Track 2 is a high-speed 125 mph passenger track with 20 to 25 million gross tons (MGT) of traffic annually that experiences track geometry degradation.

Figure 15: Geocell Installation Area

The geocell test zone is approximately 800 feet of track centered under the Oakington Road overpass, as shown in Figure 11. An additional 800+ feet of track was rebuilt, with improved drainage, but without the use of the geocell on each end of the geocell test zone.

Figure 16 presents the final design of the geocell test zone.
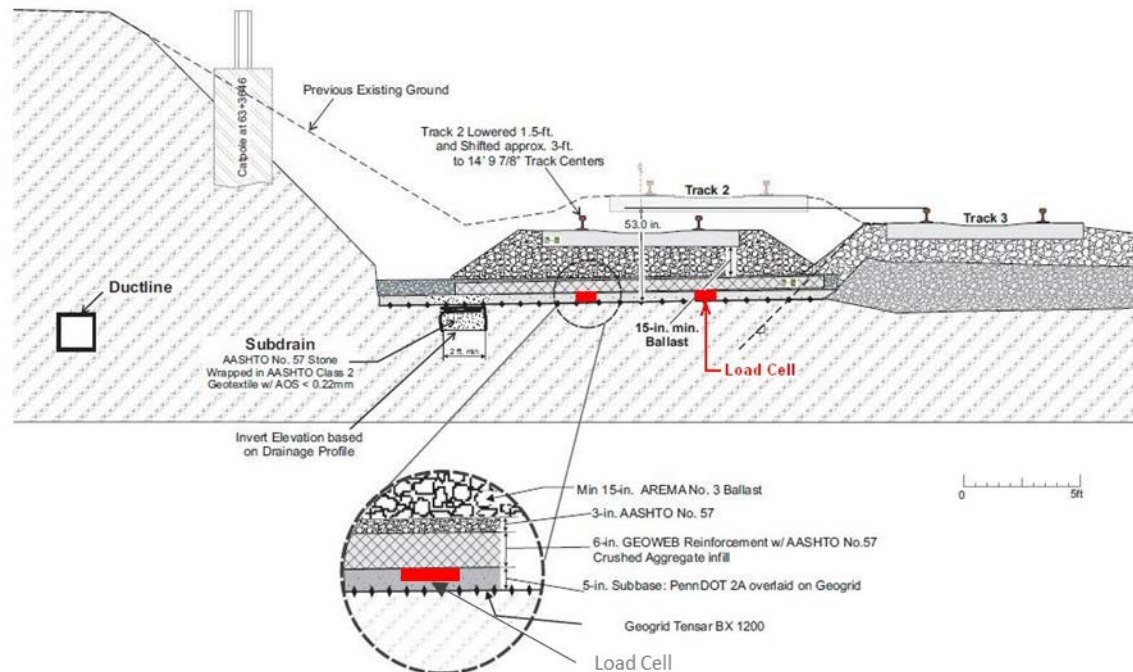
Figure 16: Final Design for Geocell Installation

As can be seen in Figure 16, there is a minimum 15 inches of AREMA No. 3 ballast under the concrete ties, above the Neoweb™ geocell material. Underneath this ballast layer and directly above the Neoweb™ geocell material is a 3-inch layer of AASHTO No. 57 sub-ballast followed by a 6 inch this layer of the Neoweb™ geocell material filled with the same AASHTO No. 57 crushed aggregate sub-ballast (see discussion and photos later in the installation section). Note the geocell layer is full track width; approximately 12 feet in width. Directly under the Neoweb™ geocell layer is an additional 5 inches of sub-ballast (PennDOT 2A) overlaid on a layer of geogrid material (Tensar BX 1200), to provide a footing for the maintenance work and to support the work equipment.

Instrumented pressure cells were inserted below the geocell layer. See the discussion below for more details.

2.1   Instrumentation

Primary instrumentation of the test zones consists of four load cells (pressure transducers) mounted as shown in Figure 16 and Figure 17. As can be seen in these figures, these load cells (pressure transducers) are located along the interface with the subgrade. The objective is to measure how much stress reduction is there due to load redistribution resulting from the geocells mattress acting as a flexible plate. The pressure transducers were installed concurrent with the installation of the geocell material, two in the unmodified sections of track (without geocell material) south of the southern end of the geocell material and two in the modified sections (with geocell material) approximately 100 feet north of the southern end of the geocell material. The force transducers were installed in the Leveling Coarse at the bottom of sub-ballast layer. One transducer was placed under each rail at the two instrumentation sections (four transducers total).

16

The two sections were at a distance approximately 230 feet (70 m) apart, and more than 100 feet (30 m) from the boundary of geocell and non-geocell zones (Figure 17). At each section, two force transducers (load cells) were used to measure the vertical pressure acting under the track at the locations of the rails. In the reinforced section, the load cells were installed under the geocell layer (Figure 16), at the same depth as in the case of unreinforced section, thus allowing for a direct comparison of measured results. A biaxial geogrid was laid under the sub-ballast layer under the geocell. The thicknesses of different layers under the track are summarized in Figure 16 and Table 1.
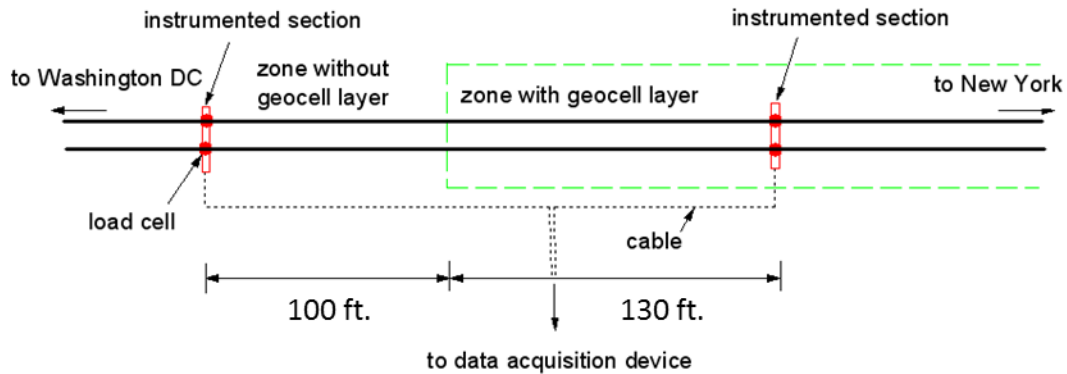
Figure 17: Plan of Instrumented Site

Table 1: Thickness of Layers Under the Track

Layer	Thickness	
	(inches)	(cm)
Ballast	15	38.1
Sub-Ballast	3	7.6
Geocell Infill Sub-Ballast	6	15.2
Sub-Base	5	12.7
Geogrid	-	-

The force transducers (pressure cells) were 8 inches (20 cm) in diameter and have a thickness of 6.6 inches (2.6 cm). They were manufactured by Tokyo Sokki Kenkyujo, Ltd. (Type KDA), see Figure 18. They have a capacity of 72 psi (500 kPa). They were installed in the sub-ballast layer directly under the geocells, as shown in Figure 16. The size was selected with consideration to the size of sub-ballasts. In the installation, a biaxial geogrid was laid with sand above it, followed by the load cell. Then, a sand bag was put over the surface of the load cells, such that the ballasts maintained a uniform contact with the surface of load cell (see Figure 29 through Figure 33 in installation section).

FORCE TRANSDUCER
Relevant for cyclic loading
Capacity: 500 kPa
Diameter: 20 cm
Thickness: 2.6 cm
Cable: length= 100 m, width=9 mm
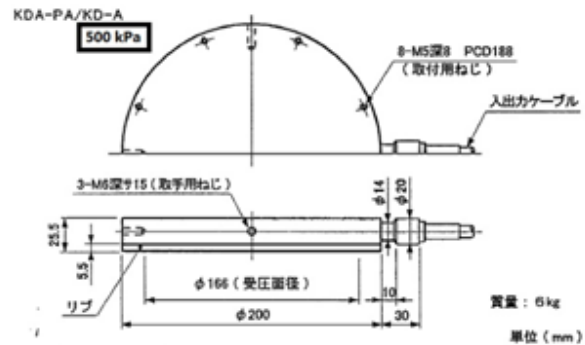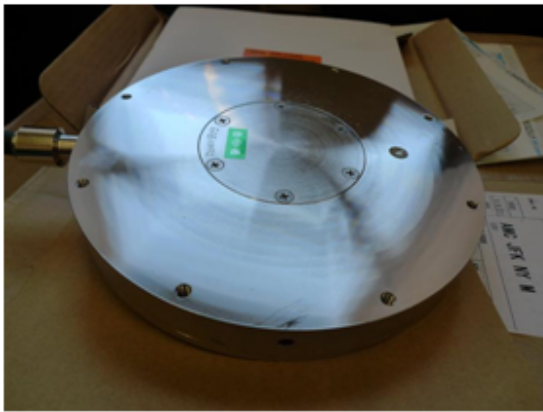
Figure 18: Force Transducer

The cables (0.354" (9 mm) diameter) connecting the load cells were buried in the ground and protected by flexible PVC conduit (1 inch (25.4 mm) in diameter) and was buried during the installation to avoid damage and vandalism. The conduit terminated at a junction box outside of the track zone, so that data recording will not require track access. Additional cabling was spooled inside the boxes to protect it between data recording sessions.

The portable data acquisition device was attached to this cabling during testing and removed when measurements were not being actively taken.   The data acquisition was conducted using a portable high-speed dynamic strain recorder DC-104A, also manufactured by Tokyo Sokki Kenkyujo, with a sampling rate of 5,000 Hz (or interval of 200 micro-second). Data logging could be controlled through a computer. Figure 19 shows the data acquisition system.

18

(a) Portable Dynamic Strain Recorder

(b) Computer Controlled Data Acquisition System

Figure 19: Data Acquisition System

3. Installation

The installation of geocell materials and load cells was conducted on September 28–30, 2015. Installation was performed by Amtrak supported by PRS Mediterranean Ltd., and the Harsco Rail and Columbia University team. Amtrak personnel performed the actual section rehabilitation to include the geocell installation, which consisted of taking the track out of service, removing the track superstructure, and the ballast/subgrade rehabilitation and upgrade (with geocell material). PRS Mediterranean Ltd., the manufacture of the Neoweb™ geocell material contributed the material, expertise, and on-site advice to Amtrak both in the design of the installation and also in the actual installation procedure.

The Columbia University team, working with Harsco and its sub-consultant (University of Delaware) installed the soil pressure transducers during the track renewal process (September 30, 2015). Figure 20 through Figure 26 documents the installation of the geocell material and rebuilding of Track 2. Figure 27 and Figure 28 show the rebuilt zones without the geocell material.

Figure 20: Compacted Sub-Ballast Layer

Figure 21: Geocell Ready for Deployment
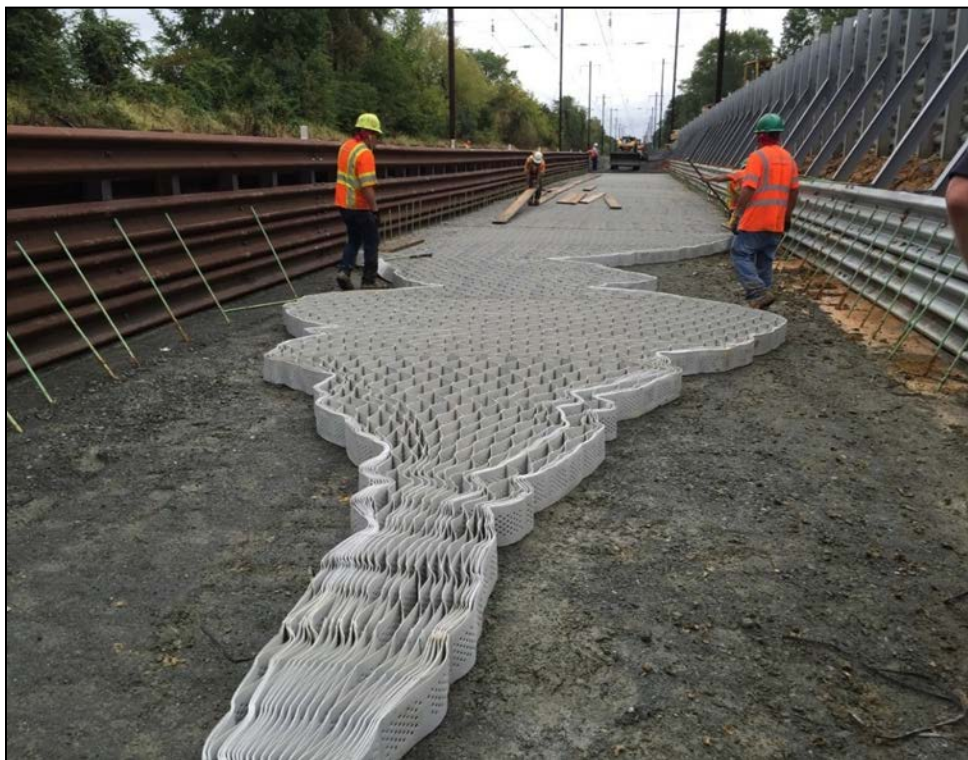
Figure 22: Opening the Neoweb™ Material

Figure 23: Opening the Neoweb™ Material

Min 15-in. AREMA No. 3 Ballast

3-in. AASHTO No. 57

6-in. GEOWEB Reinforcement w/ AASHTO No.57 Crushed Aggregate infill

5-in. Subbase: PennDOT 2A overlaid on Geogrid

Geogrid Tensar BX 1200

Load Cell
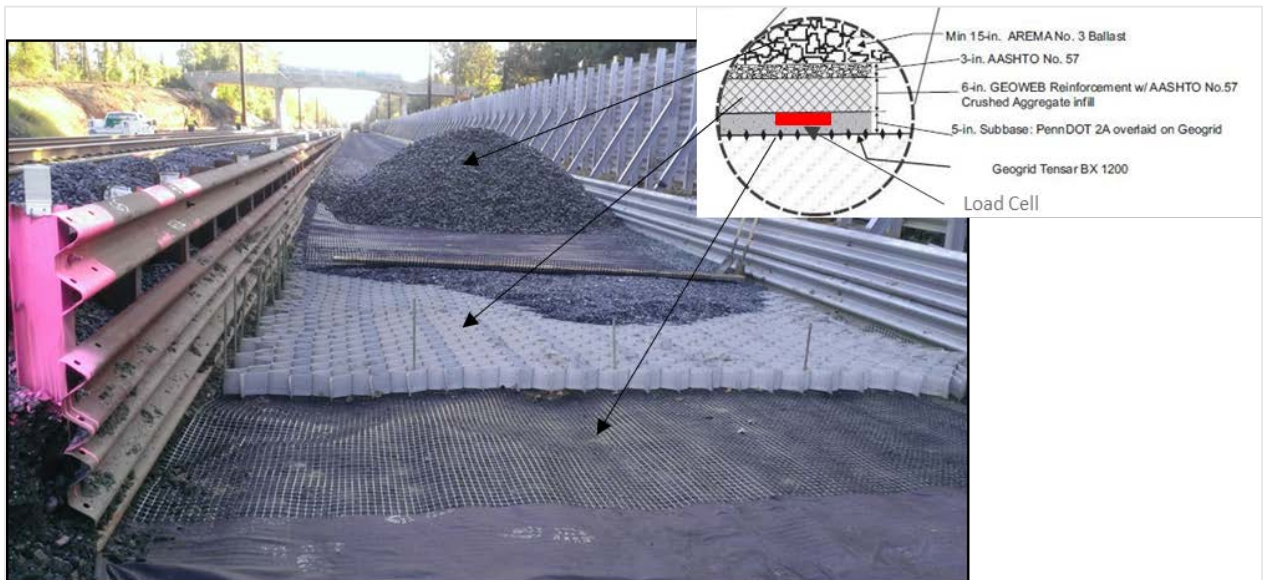
Figure 24: Filling the Neoweb™ Geocell Layer with Sub-Ballast

Figure 25: Geocell Layer and Infill Material

Figure 26: Track at Completion

Figure 27: Soil at Cut Line for Unreinforced Section

Figure 28: Overlapping Biaxial Geogrid Layers at End of Reinforced Zone

Installation of the pressure cells are shown in Figure 29 through Figure 33.

Figure 29: Load Cells Ready for Deployment

Figure 30: Load Cell with Protected Cable

Figure 31: Pressure Cell Close-Up

Figure 32: Load Cells at Locations Under the Track, Covered by Sand Bags

Figure 33: Pressure Cells in Zone Without Geocell Material

4. Monitoring of Track Geometry

Amtrak, as part of its ongoing maintenance activity (and in accordance with FRA's Track Safety Standards), operates a high-speed track geometry car on the NEC recording key track geometry data on a monthly basis. As part of this monthly inspection, the geometry car measures the key track geometry parameters to include surface (vertical), alignment (horizontal), cross-level, gauge, and twist (change in cross-level). These parameters are used to define the geometric condition of the track and to determine when the track requires maintenance (or else train traffic is slow ordered). This is clearly illustrated in the proposed test site, where Track 2 is a 125-mph track (FRA Class 7), which deteriorates to Class 6 (110 mph) or even Class 5 (90 mph). This requires slow ordering the track, i.e., imposing speed restrictions on the operating trains, until the track is surfaced and the geometry is restored.

The key track geometry parameters which are addressed by the use of the geocell technology are the vertical surface, cross-level and twist. These were recorded by the Amtrak Track Geometry Car during each of the regular (monthly) inspections and the data provided to Harsco team for analysis.

4.1 Data Collection

Upon commencement of rail service on Track 2, measurement data, to include pressure cell data (related to the four load cells) as well as track geometry data were measured and analyzed. The service was resumed on October 31, 2015. The test site was monitored for approximately 10 months to include both pressure cell and track geometry measurements.

The pressure cell monitoring plan was accomplished in several phases. In the first phase, daily measurements were taken for a week, followed by the second phase where weekly (10 days) measurements were taken for a month. In the third phase, measurements were taken on a monthly basis for a period of 6 months. The main purpose of instrumentation was to observe possible changes in results following the construction with the passages of trains.

The schedule of instrumentation is given in Table 2. A minimum of two passages were recorded each day for Northeast Regional and Acela trains given the fact that they are of different weights and also traveling at different speeds (150 mph or 240 km/h for Acela, 125 mph or 201 km/h for Regional).

Table 2: Field Instrumentation Schedule

Phase	Date	Temperature °F (low)	Temperature °C (low)
Phase 1 Daily Measurements	October 31, 2015	57.2 (39.2)	14 (4)
	November 1, 2015	66.2 (53.6)	19 (12)
	November 2, 2015	64.4 (46.4)	18 (8)
	November 3, 2015	68.0 (41.0)	20 (5)
	November 4, 2015	73.4 (44.6)	23 (7)
Phase 2 Weekly Measurements	November 13, 2015	60.8 (50.0)	16 (10)
	November 23, 2015	42.8 (30.2)	6 (-1)
	December 7, 2015	57.2 (32.0)	14 (0)
	December 16, 2015	53.6 (44.6)	12 (7)
Phase 3 Monthly Measurements	January 29, 2016	42.8 (24.8)	6 (-4)
	February 26, 2016	39.2 (30.2)	4 (-1)
	March 30, 2016	57.2 (33.8)	14 (1)
	April 20, 2016	68.0 (44.6)	20 (7)
	May 18, 2016	66.2 (51.8)	19 (11)
	June 14, 2016	78.8 (60.8)	26 (16)

Figure 34 shows the first passage of train after construction, which was a Regional train for New York.

Figure 34: The First Train Passage after Completion of Construction (October 31, 2015)

Pressure cell measurements captured by the data acquisition system are shown in Figure 35.
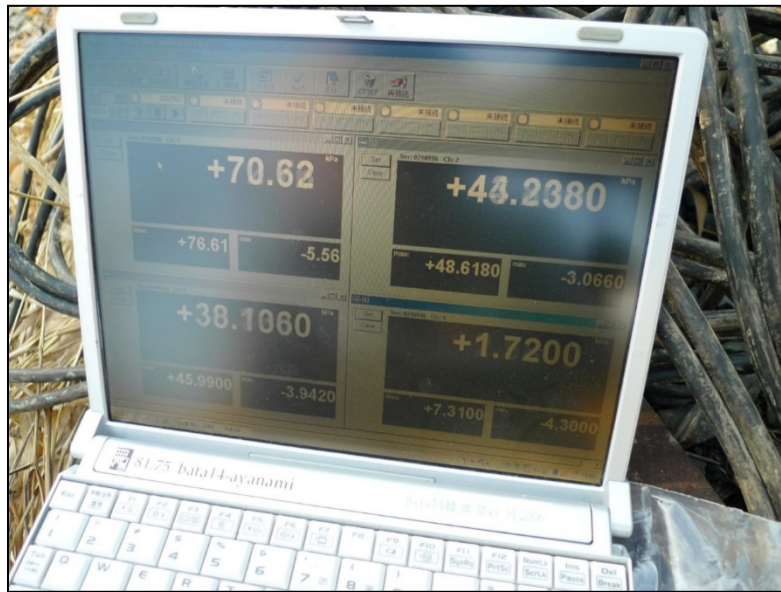
Figure 35: Pressure Cell Hardware for Pressure Cell Measurements

Track geometry measurements occurred as part of Amtrak's normal inspection scheduled and were made routinely once a month. Track geometry data was supplied for both pre- and post-geocell installation from June 2013 to the present.

5. Measurement Results and Analysis

After installation of the geocell materials and instrumentation, the performance of the test and control sites was monitored to include the key parameter of subgrade pressure and vertical track geometry. The test was monitored over a 10-month time period between November 2015 through August 2016.

5.1 Subgrade Pressure Data

As noted in the instrumentation section, subgrade pressure was monitored using four pressure cells (load cells) of which two of each where under the geocell and control sections respectively. Figure 36 shows the load cell numeral designations. Note load cells 2 and 4 are in the geocell zone and cells 1 and 3 are in the outside control zone. Load cells 2 and 3 are under the west rail and 1 and 4 under the east rail.

The results for the passage of one train as recorded by the load cells are shown in Figure 37. As can be seen from the figure, the locomotive generates higher loads than the passenger cars. The figure shows clearly that the pressure increments measured in the geocell reinforced zone (cells 2 and 4) were less than those of the unreinforced zone (cells 1 and 4). The average values acting in the reinforced and unreinforced zones were 10.3 psi (70.8 kPa) and 5.4 psi (37.2 kPa), respectively. Thus, geocell layer has resulted in a redistribution and reduction of vertical pressure by nearly half.

Figure 38 shows the results of daily and weekly measurements for Acela and Regional trains for a period of approximately 4 months after installation and resumption of service. Note, separate measurements are presented for the Acela and Regional trains because of differences in car weight and speed. The pressures increased slightly over time, but they appeared to have returned to initial value toward the end of February. Some of result variations were related to maintenance work. It can be clearly seen that the values along the left and right rails were quite consistent with the pressure measurements in the geocell zone approximately half of those for the cells in the control zone (no geocell).

Figure 39 shows the long-term results over a period of 7 months. Again, the results appear to be stable, with only slight variation, and the pressure measurements in the geocell zone approximately half of those for the cells in the control zone (no geocell).

The measurements obtained from Acela seemed more consistent compared to those of Regional trains. This may be due to larger variations in speed and passenger load for the regional trains over the 7-month time period.
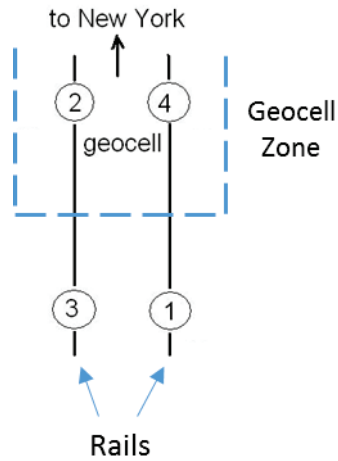
Figure 36: Load Cell Numbers and Locations
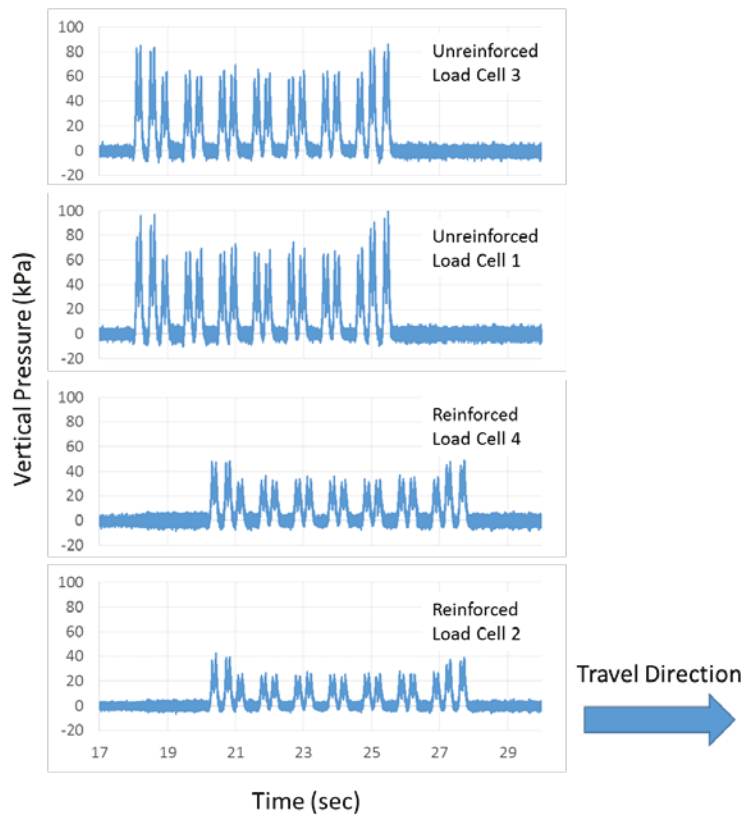
Figure 37: Load Cells and Measurements During First Train Passage
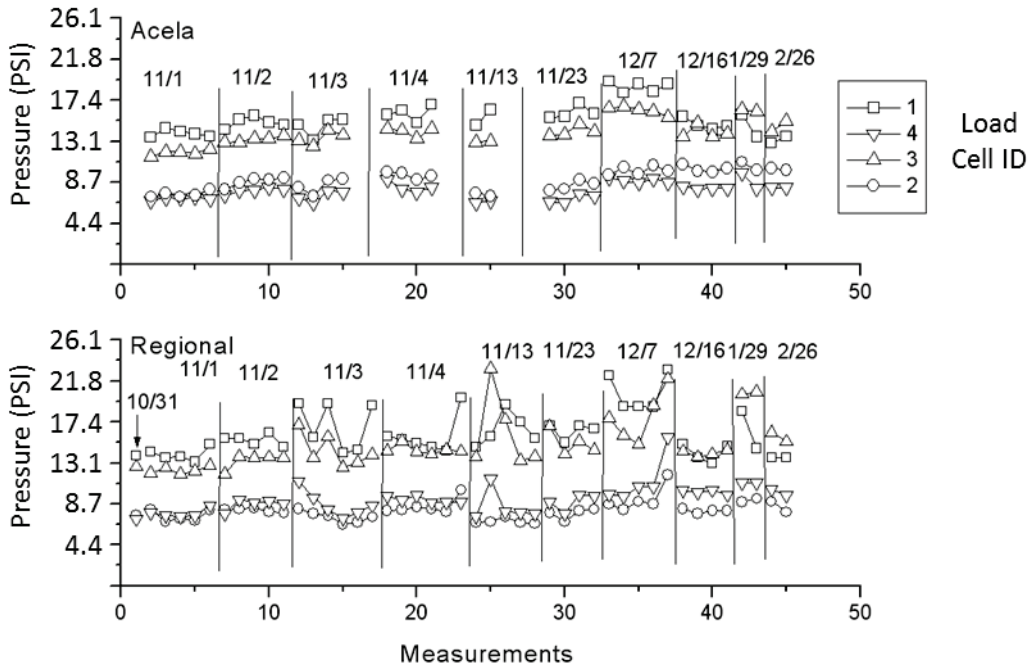
Figure 38: Pressure Cell Results of Phases 1 and 2 (4 Months)
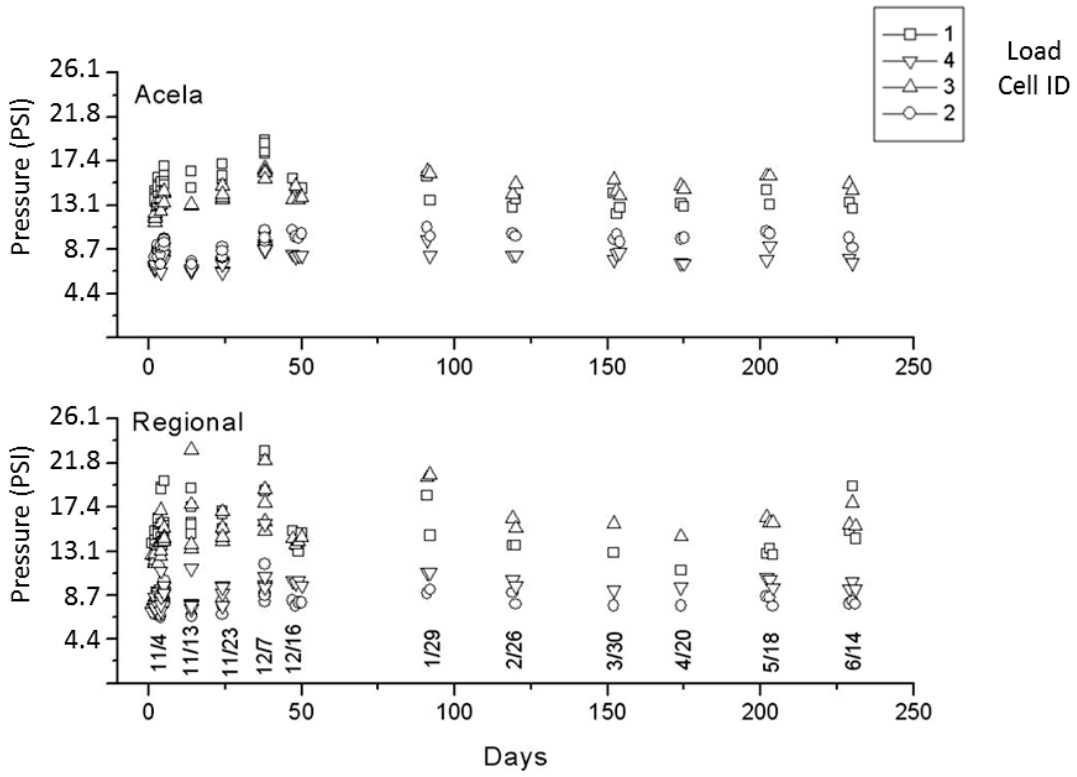
Figure 39: Pressure Cell Results Over 7 Months of Measurements

5.2 Track Geometry Measurement Data

Track geometry measurement were made using Amtrak's track geometry vehicle, which measures left and right rail surface (profile), cross-level and twist at 1 foot intervals along the track. It also records all exceptions to both Amtrak and FRA track standards.

Measurements are made monthly and data was collected as far back as 2012 (see Figure 12 through Figure 14). Figure 40 through Figure 42 present track geometry data for surface (left and right) and cross-level immediately before and immediately after the track reconstruction and geocell installation. The geocell zone is highlighted in yellow and the non-geocell zone appears on both sides of the geocell zone. Four geometry runs are presented in these figures: August 2015 (the month before the reconstruction) and January, April and June 2016, all after the reconstruction. Note, the June 2016 data is approximately 7 months after traffic resumed on the reconstructed track.

As can be clearly seen in the control zone north of the geocell zone (vicinity of MP 63.62) there were signficant geometry variations immediately before reconstruction. These were corrected during reconstruction, but by June 2016, these geometry variations reappeared at the same if not greater amplitudes. By contract, in the geocell zone, such as in the vicinity of MP 63.78, the "after" geometry variations are significantly smaller than the pre-reconstruction geometry variations, less than half the magnitude in several locations in this geocell zone. This behavior can be clearly seen in the left and right surface plots as well as in the cross-level plot (after accounting for the change in "zero" for the pre and post cross-level data.
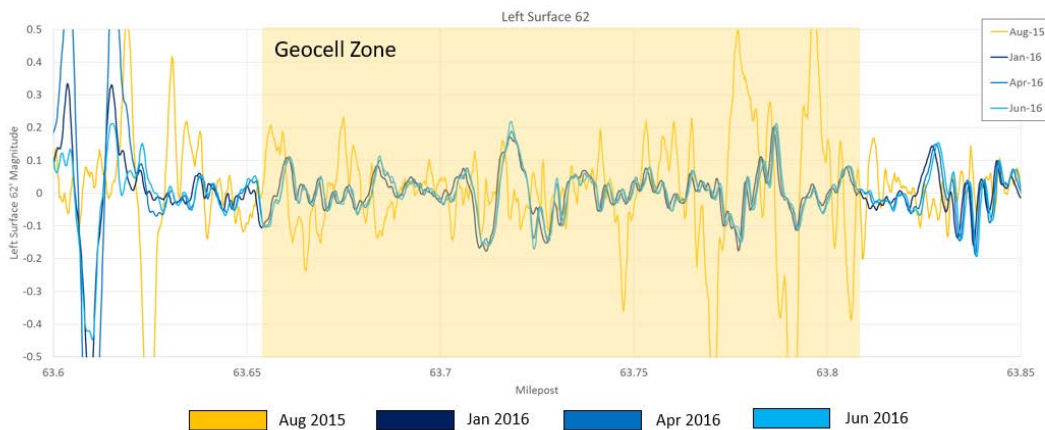
Figure 40: Pre- and Post-Installation Track Geometry Data—Left Surface (62' Chord)
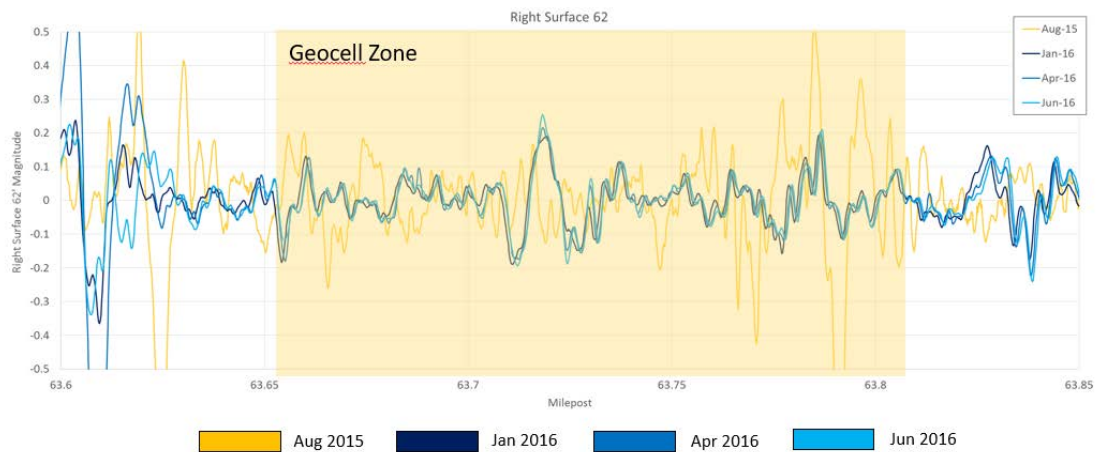
Figure 41: Pre- and Post-Installation Track Geometry Data—Right Surface (62' Chord)
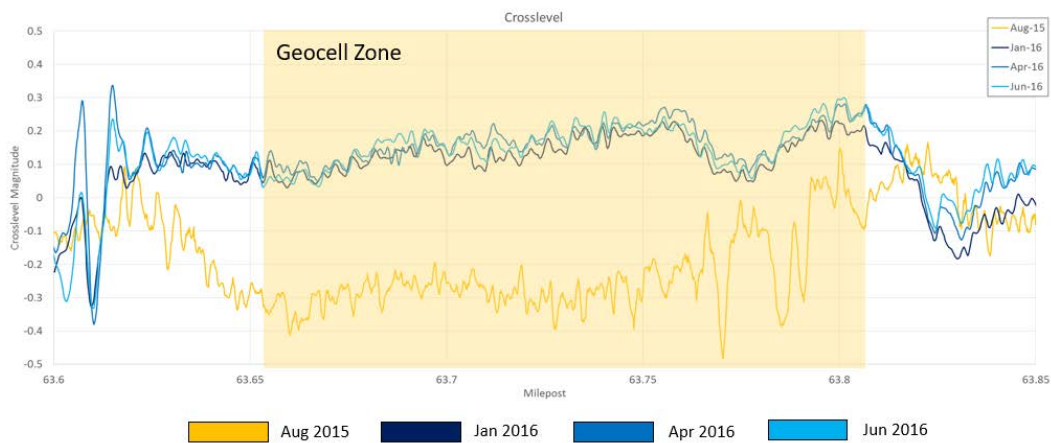
Figure 42: Pre- and Post-Installation Track Geometry Data—Cross-Level

Thus, the geocell test zone(s) clearly have a lower rate of track degradation and a correspondingly longer surfacing cycle.

This behavior is reinforced in Figure 43 and Figure 44, which shows after data through September 2016. It should be again noted that this geometry data is collected monthly.
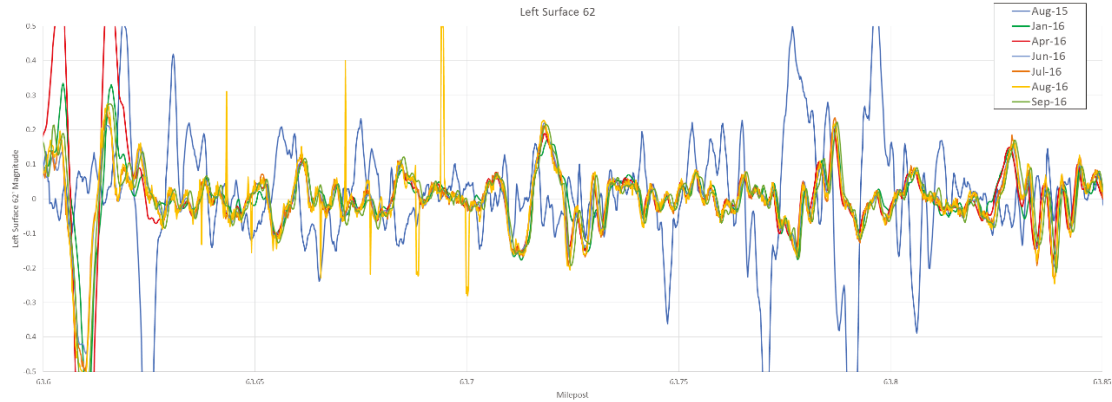
Figure 43: Left Surface 62' Through September 2016
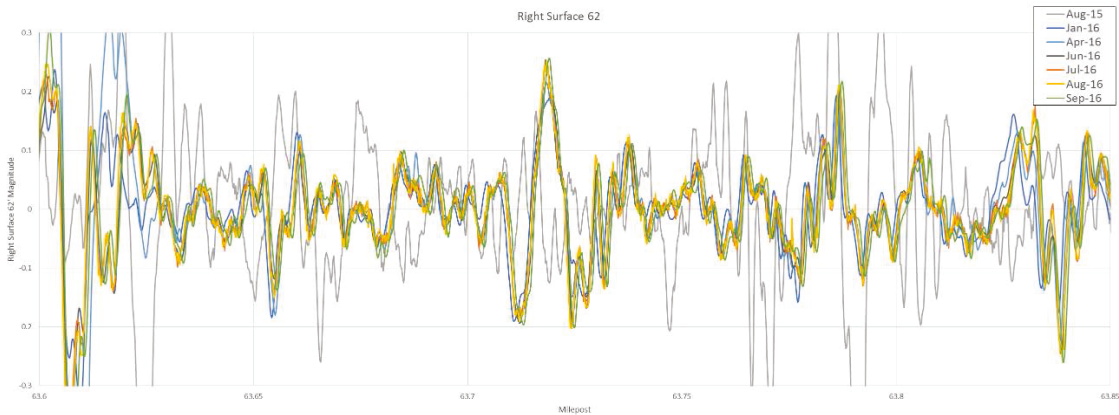
Figure 44: Right Surface 62' Through September 2016

The track geometry data was also converted to an equivalent TQI for each test zone which was calculated for each measurement cycle (monthly based on current Amtrak testing frequency) and then plotted against traffic (defined in terms of MGT of traffic). This allows for the definition of the rate of degradation of each of the test zones and serve as the basis of performance comparison.

The TQI data was calculated as follows:

- TQI was calculated for multiple channels
  - Left surface 62
  - Right surface 62
  - Cross level
- TQI defined as the standard deviation of a particular channel
- Total TQI defined as the sum of the TQI of left surface 62, right surface 62, and cross level

$$SD_{combined} = a*SD_{left\ profile} + b*SD_{right\ profile} + c*SD_{cross-level}$$

36

Where a=b=c =1

- TQI calculated:
  - Continuously
    - 50 ft moving average window
  - At various segmented window sizes:
    - 50 ft
    - 200 ft
    - 800 ft

Figure 45 presents a 50-foot moving window calculation for combined left and right surface TQI for the same four time periods as shown previously in Figure 40 through Figure 42. As seen here, the results match those presented previously with the non-geocell control zone north of the geocell zone showing high pre-reconstruction TQI values, corrected during reconstruction and then reappearing and growing even larger by 7 months after reconstruction. By contrast, the geocell zone had large pre-reconstruction TQI values which were corrected during reconstruction and has a significantly reduced rate of regrowth, such that 7 months after reconstruction the TQI values were about 1/3 the pre-reconstruction values (as opposed to the northern control zone where they exceeded the August 2015 pre-reconstruction maximum values).
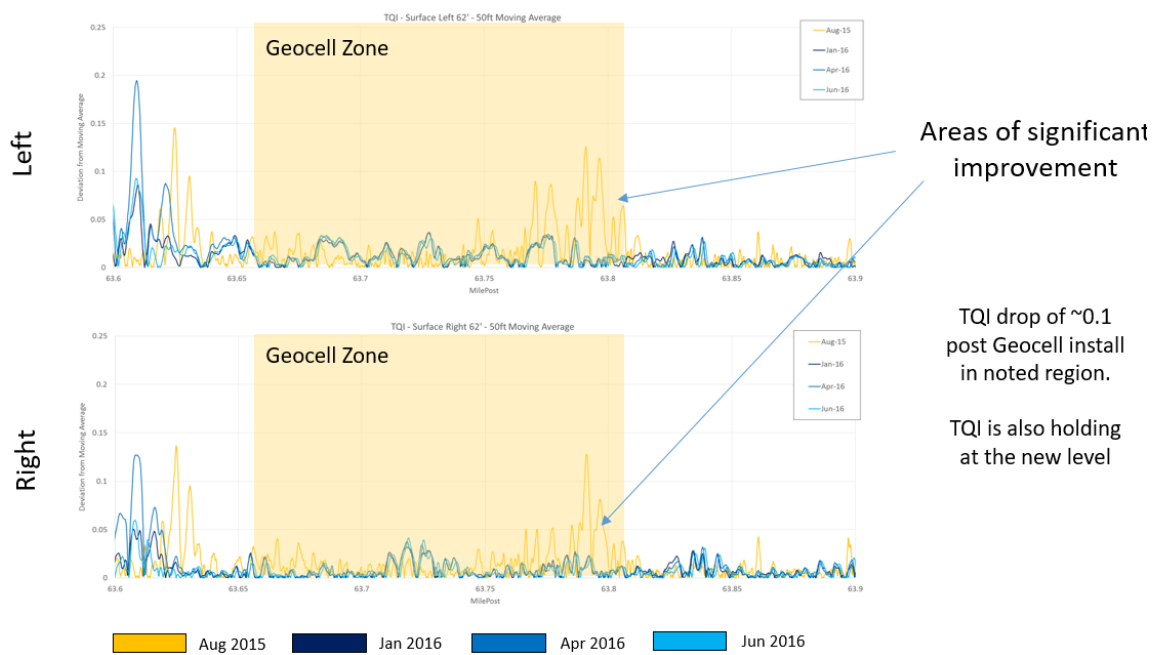
Figure 45: TQI Calculated with Moving 50-foot Window; Left and Right Surface

Figure 46 through Figure 48 present TQI data for all three measurements as a function of time, starting from September 2014 and going through June 2016 (reconstruction was September 2016). The results are quite significant.

In the northern reconstructed control zone (Figure 46), there was significant levels of TQI pre-construction, dropping to good quality track after construction (November 2015), and then reappearing and growing to levels greater than the pre-contruction levels within 6 months. The

data indciates that a follow up surfacing cycle was required and performed at that time in this zone.

By contrast, the geocell zone showed extremely good post-construction performance. This was most clearly illustrated in the geocell zone between MP 63.76 and 63.8 (Figure 47) where the high pre-reconstruction TQI values never reappeared after reconstruction and installation of the geocell material, instead remained at a very low level even 7 months after reconstruction. The rate of track degradation, in this zone, appears to be reduced by more than a factor of 3, suggesting a corresponding increase in surfacing cycles by the same factor of more than 3.

It should be further noted that the south control zone (Figure 48) did not show this level of improvement because the corresponding rate of geometry degradation for this zone was low, suggesting better subgrade support conditions here than north of the geocell zone.
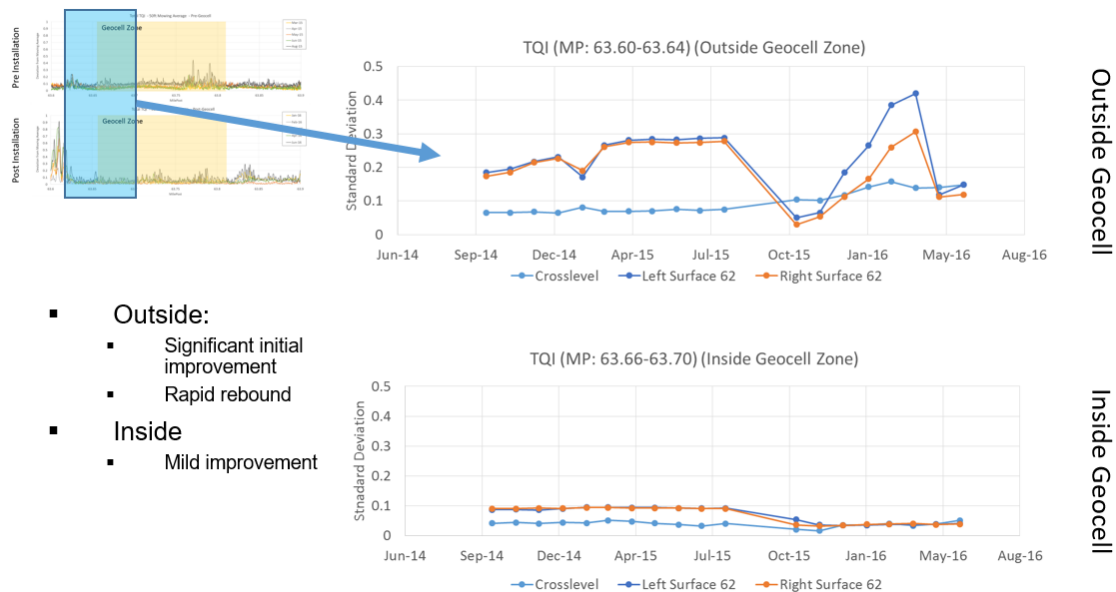
Figure 46: 200-foot Window TQI: North Control and Northernmost Geocell Zones
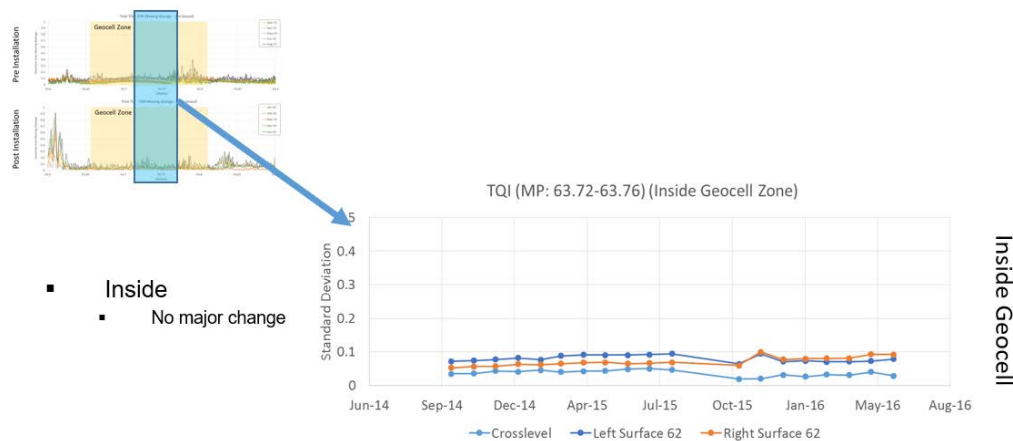
Figure 47: 200-foot Window TQI: Center Geocell Zone

- Inside
  - Significant post install improvement
  - No rebound – Improvement remains
- Outside
  - Consistent
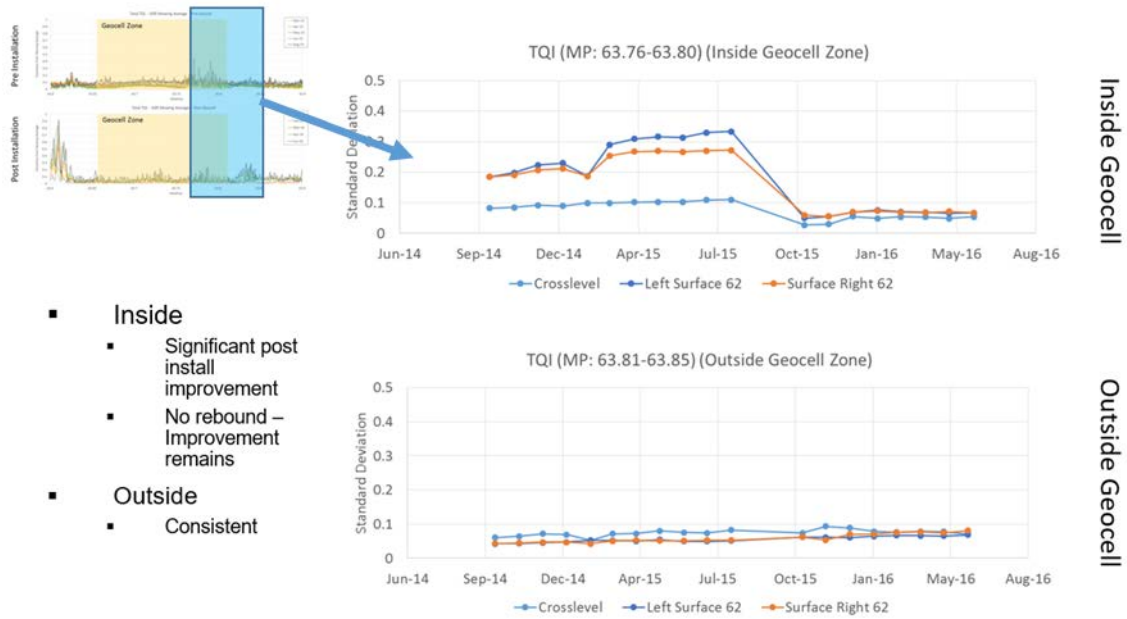
Figure 48: 200-foot Window TQI: South Control and Southernmost Geocell Zones

Figure 49 presents a "cross-mapping" of the TQI and pressure cell data for the Acela and Regional traffic, respectively. This cross-mapping is a correlation analysis between the two different sets of data. For the geocell zone, under both the left and right rails, there is a well defined relationship between lower pressure and lower TQI, corresponding to better track quality. This appears in the lower left quadrant of the graph in Figure 49. For the non-geocell zone, under both the left and right rails, there is, likewise, a well defined relationship between higher pressure and higher TQI, corresponding to poorer track quality. This appears in the upper right quadrant of the graph in Figure 49. In each of the four cases, corresponding to each one of the pressure cells, there is a linear relationship between the actual pressure and TQI values. Furthermore, this relationship appears to exist for both the Acela and the Regional traffic, through the actual loads, speeds, and pressure values are different. This data supports the previously shown results that the introduction of the geocell material improved track support, reduced bearing pressures on the subgrade and provided improved track geometry performance over time.
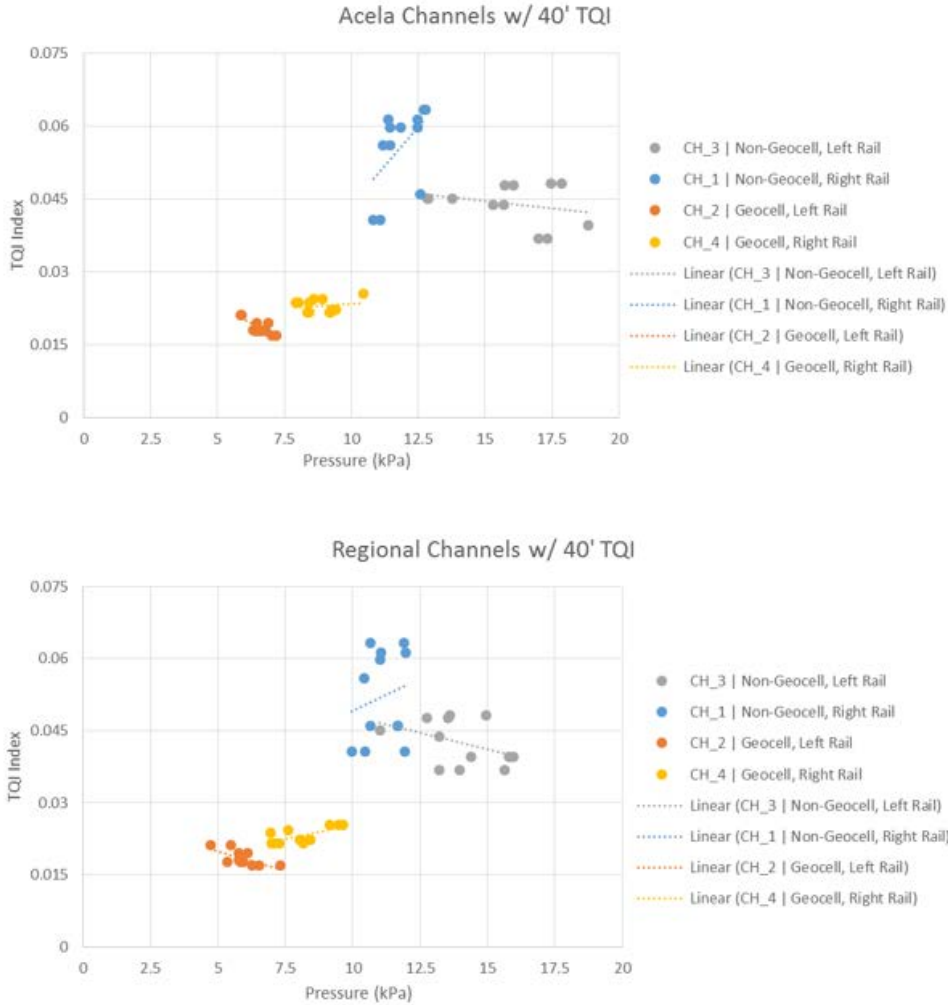
Figure 49: Cross-Mapping of Pressure and TQI Data

Figure 50 summarizes this behavior, in a manner simular to that presented in earlier, where the non-geocell zone shows the reoccurrence of rapid track geometry degradation, particularly in the area immediately to the north of the geocell zone where there appears to be a modest shift of the locaion of maximum geometry degradation northwards. Likewise, the geocell zone shows a dramatically reduced level fo geometry degradation, particularly in the southern portion fo the geocell zone.
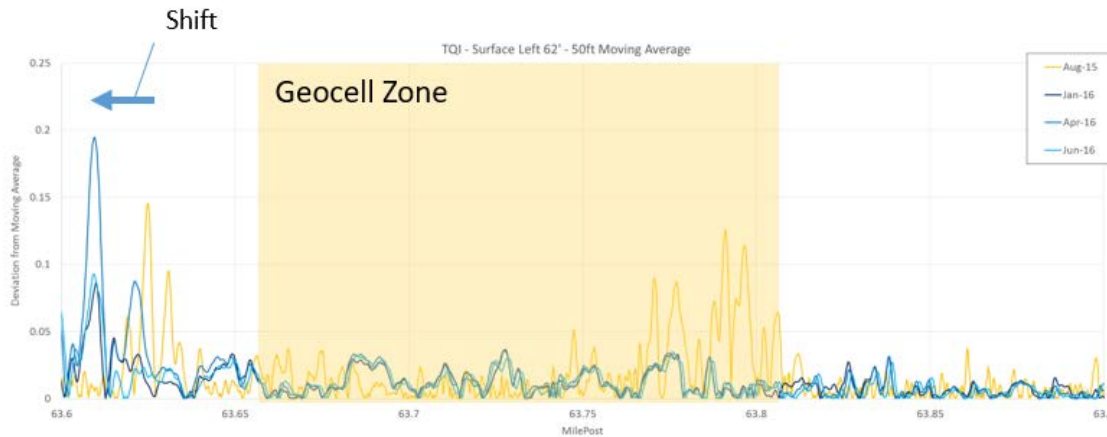
Figure 50: TQI (50' Moving Average) Before and After Reconstruction

5.3   Increase in Surfacing Cycle

One of the key determinants of the effectiveness of the geocell's reinforcement technology is the ability to reduce the rate of degradation of the track geometry. This was accomplished by analyzing the track geometry data by the Amtrak Track Geometry Car and calculating a TQI for each defined segment, as shown in the previous Figure 46 through Figure 48. The TQI used in this analysis includes the Standard Deviation (SD) of the left and right profiles (surfaces) and the Standard Deviation (SD) of the cross-level. The track degradation rate is defined by the slope of the TQI vs. the time graph as shown in Figure 51, which shows the change in TQI over time. Figure 51 represents a track segment of 200 feet, over a period of just under 2 years, with the installation of the geocell material occurring in September 2015, corresponding to the large improvement in TQI shown at that time. In addition, there was what appears to be a spot tamping (maintenance) cycle in January 2015. Looking at the left and right surface TQIs, the pre-geocell installation behavior can be seen in the period from January 2015 through August 2015 where there was a change in total TQI value of approximately 0.15 over a period of 7 months for a slope of 0.021. The post geocell installation behavior can be seen in the period October 2015 through June 2016, where there was a change in TQI value of approximately 0.25 over a period of 8 months for a slope of 0.03. The result of the geocell installation appears to be a reduction in rate of change of track geometry degradation (slope of the curve in Figure 51) of a factor of 7.
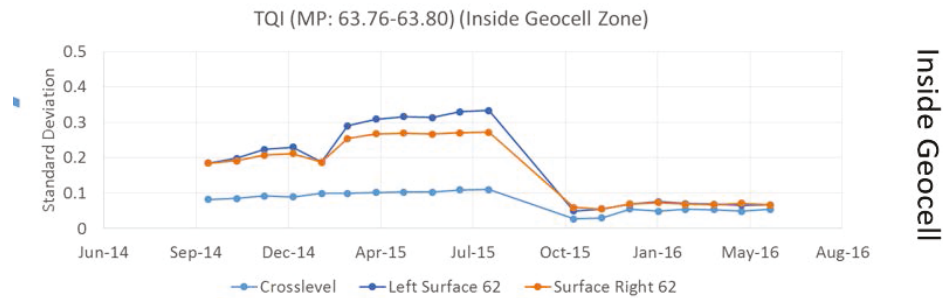
Figure 51: Track Geometry Degradation Rate Before and After Geocell Installation

Figure 52 presents the results of the combined TQIs which consists of the Standard Deviation (SD) of the left and right profiles (surfaces), the Standard Deviation (SD) of the cross-levels, combined linearly using the following equation:

$$SD_{combined} = a*SD_{left\ profile} + b* SD_{right\ profile} + c*SD_{cross\text{-}level}$$

Where a=b=c=1

For the combined TQI, the pre-geocell installation behavior can be seen in the period from January 2015 through August 2015 where there was a change in total TQI value of approximately 0.185 over a period of 7 months for a slope of 0.0265. The post geocell installation behavior can be seen in the period November 2015 through August 2016, where there was a change in TQI value of approximately 0.036 over a period of 9 months for a slope of 0.004. The result of the geocell installation appears to be a reduction in rate of change of track geometry degradation (slope of the curve in Figure 51) of a factor of 6.7.
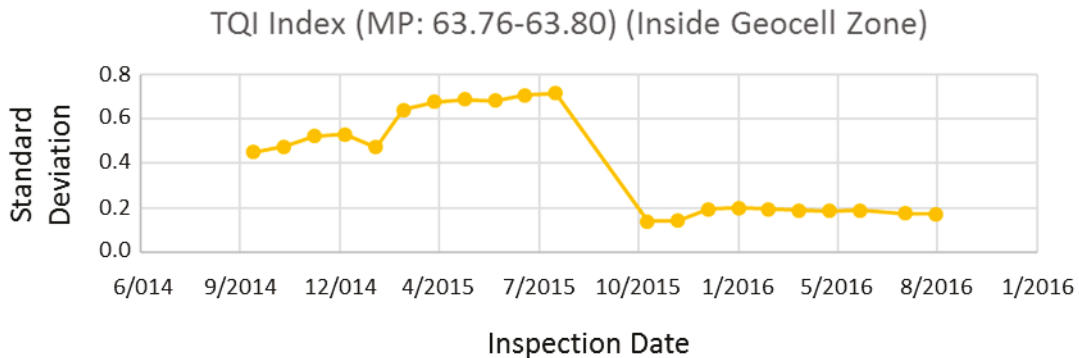
Figure 52: Combined TQI Degradation Behavior

Other parts of the geocell zone experienced smaller levels of improvement. However, it should be noted that the surfacing cycle is determined by the "worst" segment in a zone, so that the surfacing of the entire geocell zone (and most probably the entire test zone) would be set by the "worst case" 200-foot segment shown in Figure 51.

In both cases, the effect of installing the geocell material was to significantly increase the surfacing cycle by a factor of 6.7 times the pre-geocell installation surfacing cycle.

6. Economic Analysis for the Use of the Geocell Material

Since installation of geocell material has a measurable cost, an economic life cycle benefit analysis was performed to evaluate the overall economics of installing the geocell material and the resulting reduction in follow up maintenance costs due to the extended surfacing cycles. Thus, an economic analysis of the use of the geocell material was performed to assess the cost-benefit tradeoff between the reduction in maintenance (surfacing) costs as compared to the cost of the material and its installation. This analysis is a Life Cycle Cost (LCC) analysis that looks at the cumulative cost of the frequent surfacing cycles, under the 'existing' condition operations, i.e., with the high rate of track geometry degradation and frequent surfacing (corresponding to the "left" side of Figure 51), as compared to the reduced rate of surface degradation after installation of the geocell material (corresponding to the "right" side of Figure 51). The actual rates of degradation were based on the analysis of the track geometry degradation, as performed in the previous section for the pre- and post-geocell installation time periods in the defined test section. Figure 52 presents the degradation behavior for combined TQI which shows a reduction in rate of degradation after geocell installation of a factor of 6.7.

In addition, LCC sensitivity analyses were performed to examine the sensitivity of the LCC costs of the geocells implementation (and associated economic benefits) to both material and installation costs. These sensitivities provide guidance to the manufacturers and the railroads in terms of how to maximize their economic benefits using these techniques.

The economic analysis was performed used a LCC model developed for PRS Mediterranean Ltd., using Amtrak costs and operating parameters. Note, the study team validated the analysis model and the results presented here-in.

6.1 Economic Input Parameters

The following sections will detail the various inputs used in the LCC model.

6.1.1 Costs

The costs used in this analysis were based on estimates of actual costs incurred by Amtrak. It should be noted that the costs and benefits are defined on a per mile basis except as noted below. The expected costs for a section of track less than 1 mile (e.g., the Oakington Road test installation was 800 feet) is assumed to be linear, so that the corresponding ROI results will remain the same irrespective of the actual length of track. (Note, Amtrak costing indicates that there will be economies of scale associated with application to longer segments of track, while very short applications may have a higher installation cost per square foot.)

It includes the following cost areas:

- Surfacing costs
- Cost of installation of geocell material
- Train delay costs
- Cost of money

These costs will be discussed here-in:

- Surfacing costs were assumed to be $12,000 per mile. This is consistent with industry reported surfacing costs

- The cost of installation of the geocell material.

  The costs of the Neoweb™ geocell material itself, was obtained from the manufacturer PRS Mediterranean Ltd. at approximately $10 per square meter or $0.93 per square foot corresponding to a cost of approximately $60,000 per mile.

  The cost of the geogrid material used at the bottom of the rebuild section was estimated at approximately $3 per square meter or $0.28 per square foot corresponding to a cost of approximately $18,000 per mile.

  Amtrak has indicated that the cost of installation, to include both the geocell and geogrid layers, is of the order of $200+ per square yard ($22 + per square foot) for this short installation. However, it further noted that these costs would be reduced for longer installations, such as the per mile costs used in this analysis. Further noting that Amtrak had performed additional work in this area, to include draining improvement both in this zone and in the adjacent, non-geocell zones, the analysis used here as a baseline is based on an installation cost of $7.40 a square foot (excluding materials).

  The corresponding total cost of installation, to include materials and labor, came to approximately $545,000 per mile. Because of the uncertainty in this cost, a sensitivity analysis was performed on this cost of geocell installation with a range of $200,000 to $1,000,000 per mile (corresponding to $3.16 to $15.78 per square foot).

- Train delay costs
  - Train delay costs were divided into two parts:
    1. Train delay costs associated with the loss of track time due to surfacing.

    2. Train delay costs associated with poor track quality and associated with reduced track speeds, for the time between surfacing cycles.

       In both cases, train delay costs were taken to be $1,000 per train. Assuming traffic to be 25 MGT per year with an average train weight of 1,000 tons, this corresponds to approximately 3 trains per hour, and the corresponding train delay cost is $2,850 per hour.

       The corresponding train delay due to surfacing, based on a tamping rate of 20 ties per minute and concrete tie track with 2,640 ties per mile, is based on a delay of 2.2 hours per mile which comes to $6,280 per mile.

       The corresponding train delay due to slow orders on track with degraded geometry was calculated for a 0.25-mile section of slow ordered track, with a speed reduction of 30 mph (corresponding to one FRA class of track) and an acceleration and braking rate of 1 mph/sec. Assuming only 10 percent of trains are affected by this slow order and that the duration of the slow order is 5 percent of the surfacing cycle, then the cost of this train delay is approximately $18,034.

The corresponding total cost of train delay was calculated to be approximately $24,000.

- Cost of money
  - The cost of money was assumed to be 7 percent with inflation accounting for 2 percent for a net cost of money of 5 percent.

6.1.2 Surfacing Cycle

As noted previously, the surfacing cycle for the Oakington Road zone, prior to installation of the geocell material was approximately 6 months (see Figure 51). While other portions of the zone had a slower rate of geometry degradation, if surfacing has to be performed because of a poor subsection of the zone, normal practice is to surface between 0.5 and 1 miles so that the entire geocell zone would be surfaced. The base case in the analysis used a surfacing cycle of 0.5 years (6 months) which corresponded to the behavior shown in Figure 51.

However, because of the potential for variation, the sensitivity analysis was performed for surfacing cycles of between 0.5 and 3 years.

6.1.3 Surfacing Cycle Extension

The actual surfacing cycle extension, which is the same as the reduction in the rate of track geometry degradation as defined by the slope of the TQI vs. time curve (Figure 51) was calculated to be 7 for left and right profile (Figure 1) and approximately 6.7 for combined TQI. The base case in the analysis used an extension factor of 6.7.

Again, because of the potential for variation, the sensitivity analysis was performed for surfacing cycle variations of between 3 and 8.

6.1.4 Life Cycle

The life of the Neoweb™ geocell material was assumed to be 50 years. This assumption is conservative based on specification from the manufacturer.

6.2 Savings and ROI Calculation

Using the above input, the total LCCs and savings were calculated together with the ROI as shown in Table 3.

Table 3: NPV Savings Analysis

Cost per surfacing cycle			$12,000	per mile
Train delay costs			$24,313	per mile
Total surfacing costs			$36,313	per mile
Neoweb™ costs			$545,464	per mile
Neoweb™ life			50	years
Surfacing cycles:				
No geofabric		0.5		years
Neoweb™		3.4		years
Net cost of money	5.0%			
Annualized total surfacing cost:				
No geofabric			$ 75,338	per mile
Neoweb™			$ 12,041	per mile
Annual Total Surfacing Savings (No geofabric – Neoweb)			$ 63,297	per mile
Present Value			$ 1,155,545	per mile
Neoweb™ costs			$ 545,464	per mile
Annualized Neoweb™ costs			$ 29,879	per mile
Net annual savings due to Neoweb™			$ 33,418	per mile
NPV of savings			$ 610,081	per mile
ROI	112%			

The corresponding annual savings in delayed surfacing costs and avoided train delay costs came to $75,000 per mile with a Net Present Value (NPV) of approximately $1,155,000. The associated Neoweb™ material and installation costs came to $545,000 or approximately $29,879 a year. The resulting net savings was $33,418 a year with a NPV of $610,000 and an ROI of 112 percent.

Thus, for the analyzed case at Oakington Road, the economics prove to be strongly favorable for the geocell material.

6.3 Sensitivity Analysis

As noted previously, there is expected variability in several of the key inputs to include:

- Surfacing cycle
- Surfacing cycle extension
- Cost of geocell installation

As a result, a serious of sensitivity analyses were performed for these three variables.

6.3.1 Surfacing Cycle

Surfacing cycle on Amtrak NEC is expected to vary from every 6 months for very poor condition track (such as the Oakington Road section shown in Figure 1) to every 3 years for better quality track with good ballast and subgrade support conditions. The sensitivity of the surfacing costs savings (both annual and NPV) are presented in Table 4, Figure 53, and Figure 54.

As can be seen in this table and figures, for surfacing cycles of 0.5 to 2 years, the geocell shows significant economic benefit above and beyond the cost of the geocell material and installation.

Table 4: Sensitivity to Surfacing Cycle

	Annualized		cycle	Annualized		annual savings	Present Worth of Savings	NeoWeb Cost		Neoweb co
years	cost		with NeoWeb	cost		per mile	per mile			annualized
0.5	$75,338		3.35	$12,041		$63,297	$1,155,545	$545,466		$ 29,879
1	$38,128		6.70	$6,511		$31,617	$577,198	$545,466		$ 29,879
2	$19,529		13.40	$3,783		$15,746	$287,459	$545,466		$ 29,879
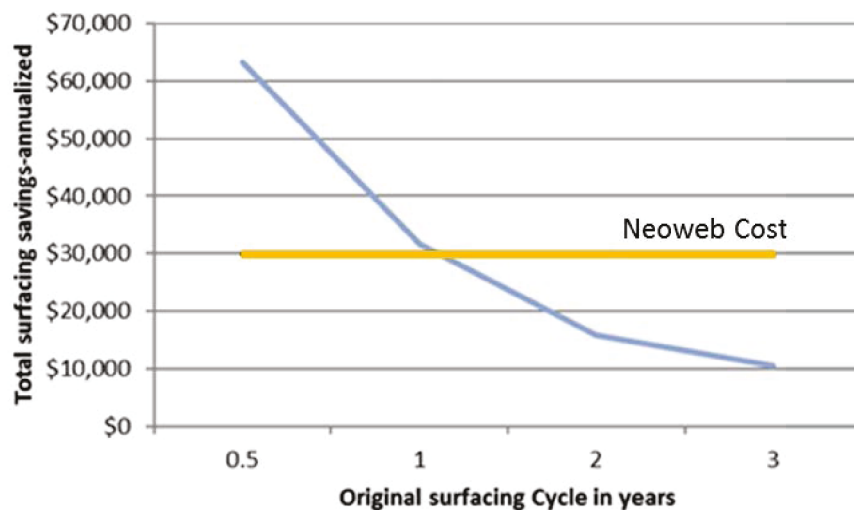
Figure 53: Sensitivity of Annual Surfacing Costs Savings to Surfacing Cycle
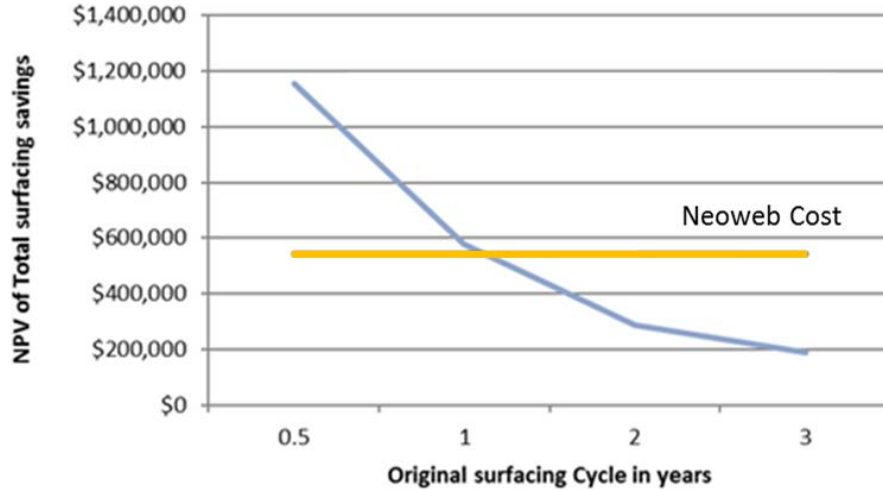
Figure 54: Sensitivity of NPV of Surfacing Costs Savings to Surfacing Cycle

6.3.2 Surfacing Cycle Extension

As noted above, the calculated surfacing cycle extension due to the installation of the geocell material at Oakington Road (see Figure 1) was a factor of 6.7. However, this was the zone with the greatest geocell effect, other zones had a lower rate of extension. As a result, a sensitivity analysis was performed for extension values ranging from 3 to 8. These results, which are presented in terms of ROI are shown in Table 5 and Figure 55.

As can be seen in this table and figure, at a surfacing life extension of 7, the ROI for the base case Oakington Road analysis is almost 113 percent.

Table 5: Sensitivity to Surfacing Cycle Extension

Surfacing Cycle (years)	Annualized Cost	Cycle Extension	Cycle w NeoWeb	Annualized Cost	Annual Savings	Present Worth of Savings per Mile	Cost of NeoWeb	ROI
0.5	$75,338	3	1.50	$25,728	$49,610	$905,681	$545,466	66%
0.5	$75,338	4	2.00	$19,529	$55,809	$1,018,840	$545,466	87%
0.5	$75,338	5	2.50	$15,812	$59,526	$1,086,709	$545,466	99%
0.5	$75,338	6	3.00	$13,334	$62,004	$1,131,933	$545,466	108%
0.5	$75,338	7	3.50	$11,566	$63,772	$1,164,216	$545,466	113%
0.5	$75,338	8	4.00	$10,241	$65,097	$1,188,412	$545,466	118%

ROI of NeoWeb (0.5 year surfacing cycle)
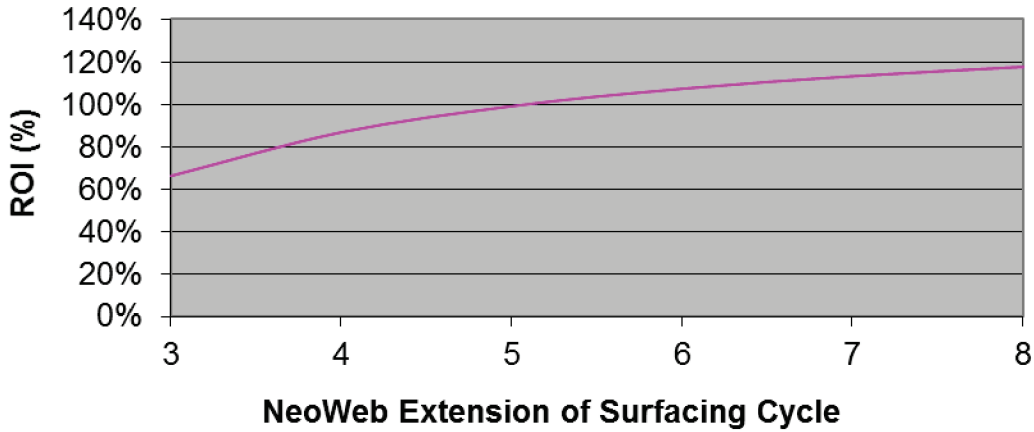
Figure 55: Sensitivity of ROI to Surfacing Cycle Extension

6.3.3 Cost of Geocell Installation

Another variable, which is not readily quantifiable, is the cost of installation of the geocell material to include the cost of the material itself and the cost of the installation. While an accurate cost for the material was obtained from the manufacturer, PRS Mediterranean Ltd., the actual cost of installation was difficult to quantify for a number of reasons. First the total project involved more than simply installing the geocell (and geogrid) material, it also involved renovation and drainage improvement for a section of track more than three times the length of the geocell zone. It was also Amtrak's first attempt to install geocell materials and as such there was a significant learning curve associated with this installation. As a result, for this analysis, a combination of manufacturer experience in other parts of the world was used, together with estimated Amtrak cost numbers to obtain the installation cost of $7.40 a square foot used in this analysis. Due to the "softness" of this number, sensitivity analysis was performed for installation costs (material plus installation) ranging from $3.16 to $15.78 per square foot corresponding to a per mile cost of $200,000 to $1,000,000. These results, which are presented in terms of ROI are shown in Table 6 and Figure 56.

As can be seen in this table and figure, at an installation cost of $545,000, the ROI for the base case Oakington Road analysis is almost 112 percent and significant ROI is obtained even if the installation cost triples from the base assumption.

Table 6: Sensitivity to Cost of Geocell Installation

years	Annualized cost	cycle extension	cycle w NeoWeb	Annualized cost		annual savings		Present Worth of Savings	Cost of NeoWeb		ROI
							years	per mile	Install	cost/sq ft	
0.5	$75,338	6.7	3.35	$12,041		$63,297		$1,155,545	$200,000	$ 3.16	478%
0.5	$75,338	6.7	3.35	$12,041		$63,297		$1,155,545	$300,000	$ 4.73	285%
0.5	$75,338	6.7	3.35	$12,041		$63,297		$1,155,545	$400,000	$ 6.31	189%
0.5	$75,338	6.7	3.35	$12,041		$63,297		$1,155,545	$500,000	$ 7.89	131%
0.5	$75,338	6.7	3.35	$12,041		$63,297		$1,155,545	$600,000	$ 9.47	93%
0.5	$75,338	6.7	3.35	$12,041		$63,297		$1,155,545	$700,000	$ 11.05	65%
0.5	$75,338	6.7	3.35	$12,041		$63,297		$1,155,545	$800,000	$ 12.63	44%
0.5	$75,338	6.7	3.35	$12,041		$63,297		$1,155,545	$900,000	$ 14.20	28%
0.5	$75,338	6.7	3.35	$12,041		$63,297		$1,155,545	$1,000,000	$ 15.78	16%
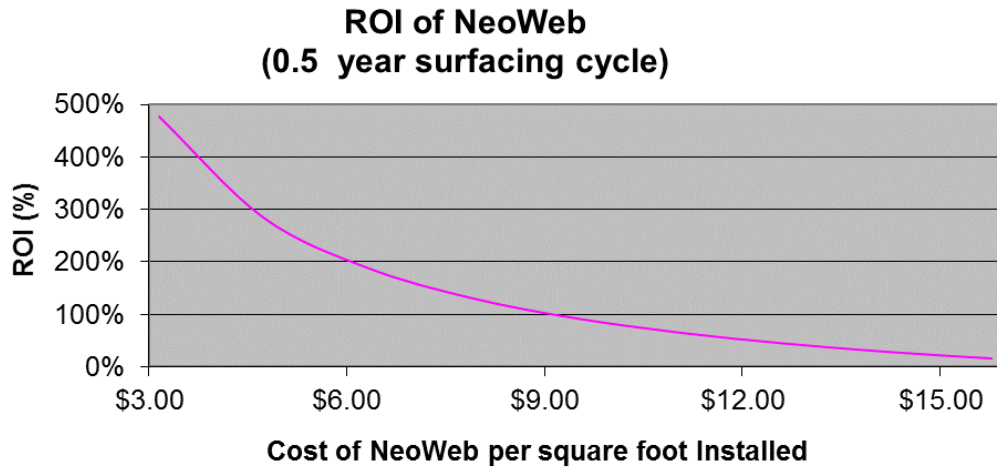
Figure 56: Sensitivity of ROI to Installation Cost of Geocell Material

7. Geocell Material and Site Post-Mortem

As part of this project, a post-mortem of the test site containing the geocell material was performed. In order to accomplish this, excavations were performed at two locations in the test zone and a section of the geocell material removed from service and sent out for testing. The purpose of the testing was to evaluate the rate of degradation of the geocell material. Testing was performed by PRS Mediterranean Ltd., the supplier of the Neoweb™ geocell material used in the test. PRS Mediterranean Ltd.'s test coordinator was Itay Asoolin, who was their envoy throughout the test program. In addition to obtaining material samples for testing, the condition of the support layers were compared to those outside the geocell zone.

Two access pits were dug and the geocell material extracted on Friday, October 21, 2016.

7.1 Digging the First Pit in an Area without the Geocell Material

The first access pit was dug in the area outside the geocell zone close to where the pressure transducers were installed. The pit was located near MP 63.9, close to the ties, on the field side of Track 2 rail (Figure 57).

Figure 57: Beginning of Pit Digging Around MP 63.9

As can be seen in Figure 58, a layer of geogrid material was installed between the ballast and sub-ballast. In addition, a layer of geotextile was installed between the sub-ballast and subgrade as shown in Figure 59.

Figure 58: Geogrid Layer Installed Between the Ballast and Sub-Ballast

Figure 59: Geotextile Layer Installed Between the Sub-Ballast and Subgrade

The subgrade was observed to be in good, dry condition, as shown in Figure 60.

Figure 60: Subgrade Condition

Upon conclusion of the field observations, the pit was closed. The onsite crew then proceeded to dig the second pit to extract the geocell material.

7.2   Digging the Second Pit in an Area with the Geocell Zone

In order to retrieve a sample of the geocell material, as close as possible to the area directly below the rail, the second pit was dug as near to the end of the tie as possible near the southern end of the geocell installation zone (approximately MP 63 + 4240). Similar to the first pit, the second pit was on the field side of Track 2. Since the ballast section in this region would take a long time to remove by hand, a backhoe was utilized to assist (Figure 61). Approximately 2 hours of foul time was necessary to dig out the ballast with the backhoe.
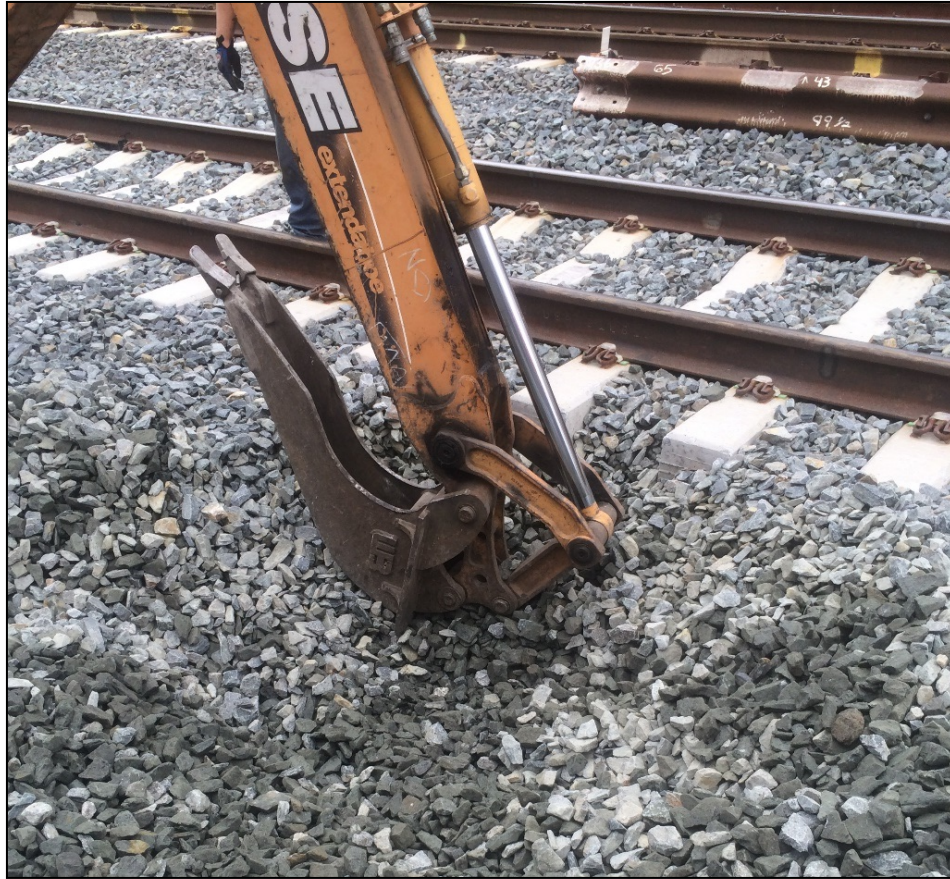
Figure 61: Utilizing a Backhoe to Dig the Second Pit on Track 2 Field Side (Geocell)

As pit depth approached the geocell layer, small hand held tools, such as a shovel, were used to avoid damage to the geocell material (Figure 62). Once the geocell layer was reached, the sub-ballast was manually removed so a sample of the geocell could be obtained (Figure 63 and Figure 64).

Figure 62: Hand Held Tools Were Used to Reach the Geocell Material Without Damaging It

Figure 63: Top Surface of Geocell Layer

Figure 64: Removing the Sub-Ballast by Hand

When the geocell was fully excavated, the edge of the geocell material was accessible, making it easier to cut out a sample (Figure 65).

Figure 65: Edge of Geocell Layer

The sample was removed utilizing a set of cutting pliers. Figure 66 and Figure 67 show the geocell sample, containing two full cells, after removal.

Figure 66: Side View of the Geocell Sample

Figure 67: Top of Geocell Sample

After removing the sample, the ballast was restored and then hand tamped, as shown in Figure 68, Figure 69, and Figure 70.

Figure 68: Covering the Pit

Figure 69: Tamping the Ballast Around the Ties

Figure 70: **Second Pit Completely Covered and Tamped**

7.3   General Site and Material Observations

During the extraction procedure, numerous visual observations of the excavation sites were
made, in addition to observations of the condition of the geocell material itself.

7.3.1 Pit Observations

One of the primary reasons for the selection of this test site was the presence of a significant
ballast/sub-ballast fouling issue. Figure 71 shows mud spot development in the maintenance
area before reconstruction of the site and installation of the geocell.

Figure 71: Historical Ballast Fouling of Track

The excavation pits dug inside and outside of the geocell zones showed a significant improvement in ballast/sub-ballast condition. In both sections, the following improvements were noted:

- The ballast and sub-ballast layers were in good condition and dry
  - Non-geocell pit: Figure 60
  - Geocell pit: Figure 63
- The subgrade below the geocell was in good condition and dry

This suggests that the added drainage and geocell layers have been successful, to date, in preventing fouling of the ballast/sub-ballast layers.

7.3.2 Geocell Observations

The geocell material was removed and initial observations were made of the condition of the material. Based on initial visual observations, the following could be stated:

- The geocell material was:
  - Intact
  - Free of deformation
  - Maintaining shape
  - Functioning as expected
- No puncturing was noted

- Appeared to be in new condition aside from surface discoloration from dirt 1 year after installation

Sample Testing

In order to more accurately and effectively asses the condition of the geocell material removed from track, the geocell sample was sent to PRS Mediterranean Ltd. for laboratory evaluation. This is to include laboratory assessment of the condition of the material, and if possible, supplement cyclic loading to determine the remaining life of the material and whether it has deteriorated more than expected. When test results are made available from PRS Mediterranean Ltd., a supplement report will be prepared.

8. Conclusion

As discussed in this report, this test program compared two distinct sets of track conditions, to include zones with and without a layer of Neocell™ geocell material. It should be noted that all measurement zones were rebuilt with improved drainage and well defined track structure and substructure (to include a well-defined depth of clean ballast). The test measurements included pre- and post-geocell track geometry measurements together with comparative subgrade pressure measurements inside and outside the geocell cell zones. Pre-installation/rebuild geometry data was available for over a year before the rebuild, while post-rebuild data encompassed a period of approximately 10 months.

The pressure cell measurements, which looked at subgrade pressure under left and right rails in both the geocell zone and the control (non-geocell) zones included measurements under both Acela high-speed trains and lower speed regional trains. In all cases, the subgrade pressures in the geocell zone were approximately half of those for the cells in the control zone (no geocell).

Track geometry measurement was made using Amtrak's track geometry vehicle which measures left and right rail surface (profile), cross-level and twist at 1-foot intervals along the track. Measurements were made monthly.

Examination of the pre-rebuild data showed there were several well defined locations in the overall test zone that experienced significant track geometry degradation with a great deal of geometry variations. These were all corrected during reconstruction.

In the zones with no geocell material, these geometry variations reappeared within 6 to 7 months with the same if not greater amplitudes. By contrast, in the geocell zone, such as in the vicinity of MP 63.78, the "after" geometry variations were significantly smaller than the pre-reconstruction geometry variations, less than half the magnitude in several locations in this geocell zone. This behavior was seen in the left and right surface plots as well as in the cross-level plot (after accounting for the change in "zero" for the pre and post cross-level data). Furthermore, the rate of geometry degradation was significantly less for the geocell zones than for the pre-geocell time periods for the exact same track, indicating the effectiveness of the geocell material in reducing the rate of track geometry degradation and extending the surfacing maintenance cycles. Analysis of the rate of degradation showed that the effect of installing the geocell material was to significantly reduce the rate of degradation (and thus increase the surfacing cycle) by a factor of 6.7 times the pre-geocell installation surfacing cycle.

9. References

Alford, S. J., and Webster, S. L. (1977). "Investigation of Construction Concepts for Pavement across Soft Ground." Report S-77-1, Soils and Pavements Laboratory, U.S. Army Engineer Waterways Experiment Station, Vicksburg, MS.

Burke, C., Ling, H. I., Matsushima, K., and Mohri, Y. (2003). "Shear Strength Parameters of Soil-Geosynthetic Interface at Very Low Confining Pressure." *Geosynthetics International*, *9*(4), 373–380.

Cardany, C., Hashimoto, H., Ling, H. I., and Sun, L. -X. (2000). "Finite Element Analysis of a Geosynthetic-Reinforced Soil Retaining Wall with Concrete-Block Facing." *Geosynthetics International*, *7*(3), 163–188.

Chrismer, S. (1997, December). "Tests of GeoWeb® to Improve Track Stability Over Soft Subgrade." AAR Technology Digest, TD 97-045.

Chrismer, S. (1999, March). "Cost Comparisons of Remedial Methods to Correct Track-Structure Instability." TTCI Technology Digest, 99–009.

Davis, D., et al. (2008, May). "Evaluation of Reinforced Ballast for Foundations in Rail Joints and Special TrackWork." TTCI Technology Digest, TD 08-019.

Grabe, H. (2010, January). "Geosynthetics for Improving Poor Track Formations." Transportation Research Board Annual Meeting.

Halahmi, I., Han, J., Leshchinsky, D., Parsons, R. L., and Pokharel, S. K. (2009). "Experimental Evaluation of Influence Factors for Single geocell-Reinforced Sand." Transportation Research Board 88th Annual Meeting, Washington, DC.

Halahmi, I., Han, J., Leshchinsky, D., Parsons, R. L., and Pokharel, S. K. (2009). "Experimental Study on Bearing Capacity of geocell-Reinforced Bases." 8th international conference on Bearing Capacity of Roads, Railways and Airfields, Urbana-Champaign, IL.

Halahmi, I., Han, J., Leshchinsky, D., Parsons, R. L., and Pokharel, P. K. (2010). "Investigation of factors influencing behavior of single geocell-reinforced base under static loading." Geotextiles and Geomembranes, *28*(6), 570–578.

Halahmi, I., Han, J., Leshchinsky, D., Manandhar, C., Parsons, R. L., Pokharel, S. K., and Yang, X.M. (2010). "Accelerated Pavement Testing of Geocell Reinforced Unpaved Roads Over Weak Subgrade." Journal of the Transportation Research Board, 2204.

Han J., Halahmi I., Pokharel S., Leshchinsky D., Manandhar C., Parsons, R., and Yang X. M. (2011, November). "Performance of geocell-reinforced RAP Bases over Weak Subgrade under Full-Scale Moving Wheel Loads." *Journal of Materials in Civil Engineering*, *23*(11).

Han, J., and Leshchinsky, D. (2006). "General Analytical Framework for Design of Flexible Reinforced Earth Structures." *Journal of Geoenvironmental and Geotechnical Engineering*, *132*(11), 1427–1435.

Han, J., Leshchinsky, D., Parsons, R. L., Rosen, A., and Yang, X. M. (2008, June 17–20). "Numerical Analysis for Mechanisms of a Geocell-Reinforced Base Under a Vertical

Load." Proceedings of the 4th Asian Regional Conference on Geosynthetics, Shanghai, China, 741–746.

Han, J., Leshchinsky, D., Parsons, R. L., and Yang, X. M. (2010). "Three-dimensional numerical modeling of single geocell-reinforced sand. " *Frontiers of Architecture and Civil Engineering in China*, *4*(2), 233–240.

Han, J., Leshchinsky, D., Parsons, R. L., Rosen, A., and Yuu, J. (2008). "Technical Review of geocells-Reinforced Base Courses over Weak Subgrade." GeoAmericas Conference Proceedings 2008, Cancun, Mexico, 1022–1030.

Kae, J. K. (2007, June). "Geotechnical and Field Measurements at Amandelbult Test Section." Spoornet (South African Railways). Technical Report.

Kalay, S., and Read, D. (1996, October). "Results of Phase II Heavy Axle Load Tests at FAST." Bulletin of the American Railway Engineering Association, Bulletin 757.

Leshchinsky, B. A., Li, L., and Ling, H., Leshchinsky, D. (2010, January). "Summary of Reinforced Embankment Tests." Columbia University, Department of Civil Engineering.

Leshchinsky, B. A., and Ling, H. (2013, February). "Effects of Geocell Confinement on Strength and Deformation Behavior of Gravel." *Journal of Geotechnical and Geoenvironmental Engineering*, *139*(2).

Leshchinsky, B. A., and Ling, H. (2013). "Numerical modeling of behavior of railway ballasted structure with geocell confinement." *Geotextiles and Geomembranes*, 36, 33–43.

Leshchinsky, B. A. (2011). "Enhancing Ballast Performance Using Geocell Confinement." GeoFrontier.

Leshchinsky, D. (2009). "On Global Equilibrium in Design of Geosynthetic Reinforced Walls." *Journal of Geotechnical and Geoenvironmental Engineering*, *135*(3), 309–315.

Leshchinsky, D. (2009). "On Global Equilibrium in Design of Geosynthetic Reinforced Walls." *Journal of Geotechnical and Geoenvironmental Engineering*, *135*(3), 309–315.

Leshchinsky, D., Kaliakin, V., Liu, H., and Ling, H. I. (2004). "Analyzing dynamic behavior of geosynthetic-reinforced soil retaining walls." *Journal of Engineering Mechanics*, *130*(8), 911–920.

Leshchinsky, D., Ling, H. I., and Wang, J. -P. (2008). Cyclic behavior of soil-structure interfaces associated with modular-block reinforced soil-retaining walls. *Geosynthetics International*, *15*(1), 14–21.

Leshchinsky, D., Meehan, C. L., and Zhu, F. (2010, February). "Required Unfactored Strength of Geosynthetic in Reinforced Earth Structures." *Journal of Geotechnical and Geoenvironmental Engineering 136*(2), 281–289.

Ling, H. I., Li, L., Napoleoni, Q., and Minno, M. (2010). "Investigation of the soil geosynthetic interface behavior through a modified direct shear apparatus." Proceedings of 9th International Conference on Geosynthetics, Guaruja, Brazil, 665–668.

Ling, H. I., Tatsuoka, F., and Wu, J. T. H. (1991). "Effectiveness of In-Membrane Test in Simulating Strength and Deformation Characteristics of Nonwoven Geotextiles Under

Operational Conditions." Proceedings of Geosynthetics '91 Conference, Atlanta, GA, 601–614.

Ling, H. I., and Whittle, A. J. (2002). "Geosynthetics in Construction." Material Encyclopedia, Elsevier.

Liu, H. and Ling, H. I. (2005). "Constitutive modeling of time-dependent monotonic and cyclic behavior of geosynthetics," Robert M. Koerner Symposium, point ASCE/ASME/ASEE Conference, Baton Rouge, LA.

PRS Mediterranean Ltd.. (2009, November). "Neoweb™ Rail Track Structure Reinforcement: Technical Overview."

Abbreviations and Acronyms

FRA	Federal Railroad Administration
GPR	Ground Penetrating Radar
LCC	Life Cycle Cost
HDPE	High Density Polyethylene
MP	Milepost
MGT	Million Gross Tons
NPV	Net Present Value
NEC	Northeast Corridor
NPA	Novel Polymeric Alloy
ROI	Return on Investment
SD	Standard Deviation
TQI	Track Quality Index
TTCI	Transportation Technology Center, Inc.